

DEVELOPMENT OF DUAL-LAYER HOLLOW FIBER WITH MODIFIED
ELECTROLYTE FOR MICRO-TUBULAR SOLID OXIDE FUEL CELL

SITI MUNIRA BINTI JAMIL

UNIVERSITI TEKNOLOGI MALAYSIA

**DEVELOPMENT OF DUAL-LAYER HOLLOW FIBER WITH MODIFIED
ELECTROLYTE FOR MICRO-TUBULAR SOLID OXIDE FUEL CELL**

SITI MUNIRA BINTI JAMIL

**A thesis submitted in fulfilment of the
requirements for the award of the degree of
Doctor of Philosophy (Gas Engineering)**

**Faculty of Chemical and Energy Engineering
Universiti Teknologi Malaysia**

JANUARY 2017

In the Name of ALLAH, The Most Gracious and The Most Merciful

Specially dedicated to my beloved husband

(Ahmad Taufiq Abd Jaafar)

my children

(Muhammad Al-Fateh, Solahuddeen Al Ayyubi)

my parents

(Jamil Kasa, Che Amah Abd Kadir)

siblings

(Rosli, Siti Norjuita, Mohd Fitri, Mohd Haikal Hakim)

in-laws

(Abd Jaafar Shafie, Masri Osman,

Ruqayyah, Salahuddin, Atiqah, Muhammad, Nawal, Salman, Najihah)

and friends for their continuous support and

encouragement throughout this study

ACKNOWLEDGEMENT

Alhamdulillah, first and foremost I thank to Allah the Almighty for his Grace, Mercy and Guidance that awarded me the strength to accomplish this three and a half years of study.

Secondly, I would like to express my sincere appreciation and gratitude to my supervisor, Dr Mohd Hafiz Dzarfan, a prolific researcher in Solid Oxide Fuel Cell for his guidance, precious advice and continuous support throughout this study. Same goes to my co-supervisors Dr Juhana, an expert in Direct Methanol Fuel Cell and Dr Mukhlis, a skillful researcher in Ceramic Membrane for kindly sharing their extensive knowledge and expertise.

In addition, I would like to acknowledge Prof Dr Yugi Iwamoto, Prof Dr Masaki Tanemura (Nagoya Institute of Technology, Japan) and Sakura Science Club, for kindly providing me assistance with the sample analysis during the attachment. I am also indebted to Prof Dr Kang Li (Imperial College, London) for his valuable suggestion during this study. Special thanks to Advanced Membrane Technology Research Center (AMTEC) members for the technical supports and assistances. Extended thanks dedicated to Prof Dr Ahmad Fauzi Ismail (Director of AMTEC), Dr Zamri, Dr Maizura, Dr Farhana, Dr Nadzirah, Mrs Halimah, Ms Norfazliana, Ms Norfadhilatuladha, Ms Siti Khadijah, Ms Norazureen, Ms Huda, Ms Zanariah, Mr Azuwa, Mr Muhazri, Mr Hilmi and many others whom I have not mentioned here, for the supports, encouragement and prayers.

I also owe a special debt of gratitude to Ministry of Education Malaysia for MyPhD (MyBrain15) scholarship and Ministry of Science, Technology and Innovation Malaysia (MOSTI) for their financial support during the course of my study.

My unlimited appreciation goes to my family for their prayers, irreplaceable encouragement and understanding. Also a special thanks to my husband, Taufiq who has accompanied me even in the hardest time, for his love, patience and emotional support. My boys; Fateh and Solah whose inspired me to work even harder to achieve higher academic values, to contribute more to the community and endeavor to become a better rounded person. Lastly, I am grateful to those who have directly or indirectly assisted me in the preparation of this thesis and I hope it will be beneficial to Islam and ummah.

ABSTRACT

The excellent ionic conductivity at temperature ranges from 400-700 °C has made cerium gadolinium oxide (CGO) as one of promising alternative solid electrolyte materials for intermediate temperature solid oxide fuel cell (IT-SOFC) application. However, the requirement of high sintering temperature up to 1550 °C for densification of CGO electrolyte complicates the cell fabrication process as it reduces the porosity in the electrode layers, particularly in the co-sintering step of anode/electrolyte dual-layer hollow fiber (DLHF). Hence, the fabrication of the DLHF is challenging due to the different sintering behaviors of the each layer. The main objective of this study is to develop anode/electrolyte DLHFs with improved electrolyte properties with reduced co-sintering temperature for IT-SOFCs via a single-step phase inversion-based co-extrusion/co-sintering technique. The sintering properties of electrolyte flat sheet was studied by comparing two approaches, (i) using mix particle size electrolyte and (ii) addition of lithium oxide as sintering additive in the electrolyte. The DLHF with modified electrolyte was later fabricated by phase inversion based co-extrusion and co-sintered at temperature ranging from 1400 to 1500 °C. The DLHF was evaluated in term of the morphology, mechanical strength and gas-tightness as well as electrical conductivity, porosity and permeability of the anode layer. This study showed that a dense CGO flat sheet layer sintered at 1450 °C with the addition of 30% nano size CGO particles were obtained. Meanwhile, the doping of 2 mol% of lithium nitrate into CGO was found to reduce the sintering temperature to 1400 °C. When the co-sintering temperature increased, the mechanical strength, gas-tightness and electrical conductivity were increased, whereas the porosity and permeability of the anode layer were decreased. The DLHF that was co-sintered at 1450 °C showed sufficient properties and therefore, it was chosen for the construction of micro-tubular SOFC (MT-SOFC). When comparing the maximum power density of MT-SOFC namely nickel (Ni)-CGO/CGO (unmodified), Ni-CGO/30%nano-70%micron CGO (first approach) and Ni-CGO/lithium (Li)-CGO (second approach); it was found that the Ni-CGO/30%nano-70%micron CGO cell performed the best. At 500 °C, the cell produced the highest maximum power density, which was 275 Wm⁻² as compared to Ni-CGO/Li-CGO cell (60 Wm⁻²) and Ni-CGO/CGO cell (200 Wm⁻²). Porous anode in Ni-CGO/30%nano-70%micron CGO DLHF provided active reaction site, while dense electrolyte layer resulted from pore filling caused by the introduction of 30% nano sized CGO particles improved the gas-tightness of the electrolyte. Meanwhile, the closed pore caused by the migration of Li ions in anode sponge-like region of Ni-CGO/Li-CGO hindered the triple phase boundary region that impaired the cell performance. This limited the inclusion of Li in DLHF design. Nevertheless, the results from this study has proven the feasibilities to accelerate the densification of electrolyte as well as presented an advanced electrolyte material for MT-SOFC.

ABSTRAK

Kekonduksian ionik yang sangat baik pada julat suhu antara 400-700 °C telah menjadikan cerium gadolinium oksida (CGO) sebagai bahan alternatif elektrolit pepejal untuk penggunaan sel bahan api pepejal teroksida (IT-SOFC). Walau bagaimanapun, keperluan suhu pensinteran yang tinggi sehingga 1550 °C untuk pemadatan CGO telah merumitkan proses fabrikasi sel kerana mengurangkan keliangan dalam lapisan elektrod terutamanya dalam langkah pensinteran bersama anod/elektrolit gentian geronggang dwi lapisan (DLHF). Oleh itu, fabrikasi DLHF adalah mencabar berikutan perbezaan kelakuan pensinteran dalam setiap lapisan. Objektif utama kajian ini adalah untuk membangunkan anod/elektrolit DLHF dengan ciri elektrolit yang lebih baik dan mengurangkan suhu pensinteran untuk IT-SOFCs melalui teknik langkah tunggal songsangan fasa bersama penyemperitan dan pensinteran. Sifat pensinteran kepingan rata elektrolit telah dikaji dengan membandingkan dua pendekatan; (i) menggunakan elektrolit dengan saiz partikel bercampur dan (ii) penambahan litium oksida sebagai bahan tambahan pensinteran dalam elektrolit. DLHF dengan elektrolit yang diubahsuai kemudiannya dihasilkan dengan teknik songsangan fasa bersama penyemperitan dan pensinteran pada suhu antara 1400-1500 °C. DLHF ini dinilai dari segi morfologi, kekuatan mekanikal dan keketatan gas serta kekonduksian elektrik, keliangan dan kebolehtelapan lapisan anod. Didapati lapisan kepingan rata CGO padat yang disinter pada 1450 °C dengan tambahan 30% zarah CGO saiz nano dapat diperolehi. Sementara itu, pengedapan 2 mol% litium nitrat ke dalam CGO telah menurunkan suhu pensinteran kepada 1400 °C. Apabila suhu pensinteran bersama meningkat, kekuatan mekanikal, keketatan gas dan kekonduksian elektrik meningkat manakala keliangan dan kebolehtelapan lapisan anod berkurangan. DLHF yang telah disinter bersama pada suhu 1450 °C menunjukkan ciri yang mencukupi dan oleh itu, telah dipilih untuk pembinaan tiub mikro SOFC (MT-SOFC). Dengan membandingkan ketumpatan kuasa maksimum MT-SOFC iaitu nikel (Ni)-CGO/CGO (tidak diubahsuai), Ni-CGO/30% nano-70% mikron CGO (pendekatan pertama) dan Ni-CGO/litium (Li)-CGO (pendekatan kedua); didapati sel Ni-CGO/30% nano-70% mikron CGO menunjukkan prestasi terbaik. Pada 500 °C, sel tersebut menghasilkan ketumpatan kuasa maksimum yang paling tinggi iaitu 275 Wm⁻² berbanding sel Ni-CGO/Li-CGO (60 Wm⁻²) dan Ni-CGO/CGO (200 Wm⁻²). Anod berliang dalam sel Ni-CGO/30% nano-70% mikron CGO menyediakan tapak tindakbalas aktif manakala lapisan elektrolit padat terhasil daripada pengisian liang dengan pengenalan 30% zarah CGO bersaiz nano telah meningkatkan keketatan gas elektrolit. Manakala liang tertutup disebabkan oleh perpindahan ion Li dalam kawasan anod bagi sel Ni-CGO/Li-CGO telah menghalang rantau sempadan tiga fasa yang menjejaskan prestasi sel. Ini telah menghadkan penglibatan Li dalam reka bentuk DLHF. Walau bagaimanapun, hasil kajian ini telah membuktikan kebolehlaksanaan untuk mempercepatkan pemadatan elektrolit dan juga mengemukakan bahan elektrolit termaju untuk MT-SOFC.

TABLE OF CONTENTS

CHAPTER	TITLE	PAGE
	DECLARATION	ii
	DEDICATION	iii
	ACKNOWLEDGEMENT	iv
	ABSTRACT	v
	ABSTRAK	vi
	TABLE OF CONTENTS	vii
	LIST OF TABLES	xii
	LIST OF FIGURES	xiv
	LIST OF ABBREVIATIONS	xx
	LIST OF SYMBOLS	xxii
	LIST OF APPENDICES	xxiv
1	INTRODUCTION	1
	1.1 Research Background	1
	1.2 Problem Statement	9
	1.3 Objectives and Scopes	11
	1.4 Significance of Study	12
	1.5 Thesis Organisation	12
2	LITERATURE REVIEW	15
	2.1 Introduction	15
	2.2 Recent Fabrication Techniques for micro-tubular SOFCs Support	16
	2.3 Conventional Extrusion Technique	17
	2.3.1 Single Extrusion	18

2.3.2	Co-extrusion	32
2.4	Phase Inversion-Based Extrusion Technique	34
2.4.1	Basic Concept of the Technique	34
2.4.2	Single-layer Extrusion	37
2.4.2.1	Electrolyte-supported hollow fiber	37
2.4.1.2	Anode-supported hollow fiber	40
2.4.3	Multi-Layer Extrusion	46
2.5	Comparison between ram extrusion and phase inversion based co-extrusion	61
2.6	Reducing the electrolyte sintering temperature	63
2.6.1	Particle Size Approach	63
2.6.2	Sintering Additives Approach	66
2.7	Conclusion	70
3	METHODOLOGY	72
3.1	Introduction	72
3.2	Materials	77
3.3	Design of Experiment	78
3.3.1	Preparation of Suspensions using Mix Particle Size of CGO	78
3.3.2	Preparation of Lithium doped CGO Powders and Suspensions	79
3.3.3	Preparation of Electrolyte Flat Sheet	80
3.4	Characterization of Powders	80
3.5	Characterization of the Flat sheet	82
3.6	Preparation of Dual-layer Hollow Fiber by Co-extrusion/co-sintering Technique	83
3.7	Characterization of the dual-layer hollow fiber	86
3.7.1	Scanning Electron Microscope (SEM)	86
3.7.2	Three-point Bending	86
3.7.3	Mercury Intrusion Porosimetry	87
3.7.4	Gas Permeation and Gas Tightness	87
3.7.5	Electrical Conductivity	89
3.8	Micro-tubular SOFC Test	90

4	ELECTROLYTE MODIFICATION USING MIX PARTICLE SIZES	93
4.1	Introduction	93
4.2	Results and Discussions	93
4.2.1	Particles Behaviour	93
4.2.2	Morphologies, Surface Roughness and Mechanical Strength of Flat Sheet	100
4.2.3	Morphologies, Mechanical Strength and Gas Tightness of Dual-Layer Hollow Fibers	104
4.4	Conclusion	109
5	ELECTROLYTE MODIFICATION BY ADDITION OF LITHIUM OXIDE AS SINTERING ADDITIVE	111
5.1	Intoduction	111
5.2	Results and Discussions	112
5.2.1	Thermal decompositions of LiNO_3 and Li-CGO powders	112
5.2.2	Shrinkage Analysis of Li-CGO powders	114
5.2.3	Insight observation of Li-CGO powders	116
5.2.4	XPS analysis of Li-CGO electrolyte precursor	117
5.2.5	Effect of calcination temperature on the crystallinity of Li-CGO powders	121
5.2.6	Effect of calcination temperature on the surface area of Li-CGO	122
5.2.7	Effect of calcination temperature on the chemical interaction in Li-CGO powders	123
5.2.8	Effect of sintering additive on electrolyte suspension	125
5.2.9	Effect of sintering additive on microstructure of CGO electrolyte	128
5.3	Conclusion	133

6	DUAL-LAYER HOLLOW FIBER FABRICATION WITH ADDITION OF ELECTROLYTE SINTERING ADDITIVE	134
	6.1 Introduction	134
	6.2 Results and Discussions	134
	6.2.1 Fabrication of NiO-CGO/Li-CGO dual-layer hollow fiber precursors	134
	6.2.2 Morphological study of Ni-CGO/Li-CGO dual-layer hollow fiber	139
	6.2.3 Mechanical strength and gas tightness properties of Ni-CGO/Li-CGO dual-layer hollow fiber	142
	6.3 Conclusion	145
7	MICRO-TUBULAR SOLID OXIDE FUEL CELL DEVELOPMENT	146
	7.1 Introduction	146
	7.2 Results and Discussions	147
	7.2.1 Anode Properties	147
	7.2.1.1 Pore Distribution and Porosity of Anode	147
	7.2.1.2 Permeation and Mechanical Strength of the Anode Hollow Fiber	150
	7.2.1.3 Electrical Conductivity of Anode at Different Sintering Temperatures	152
	7.2.2 Comparison of Dual-layer Hollow Fibers Properties using Different Modification Approaches	154
	7.2.2.1 Morphological Studies	154
	7.2.2.2 Mechanical Strength and Tightness Properties	157
	7.2.2.3 MT-SOFC Performance	158
	7.3 Conclusion	164

8	CONCLUSIONS AND RECOMMENDATIONS	165
8.1	General Conclusions	165
8.1.1	Modification of the Sintering Properties of CGO Electrolyte Flat Sheet	165
8.1.2	Development of an Anode/electrolyte Dual-layer Hollow Fiber	166
8.1.3	Properties of Anode/electrolyte Dual-layer Hollow Fiber	167
8.1.4	Electrochemical Performance of Micro-tubular SOFC	167
8.2	Recommendations for Future Works	168
8.2.1	Submicron size of CGO particles	169
8.2.2	Varying the sintering additive loading	169
8.2.3	Anode Functional Layer	169
8.2.4	Bi-layer electrolyte	170
8.2.5	Dual-layer hollow fiber with thinner electrolyte	170
	REFERENCES	171
	Appendices A-B	194-197

LIST OF TABLES

TABLE NO.	TITLE	PAGE
1.1	Fuel Cell Types (U.S Department of Energy)	2
1.2	Comparison between YSZ and CGO systems	7
2.1	Recent development of single micro-tubular SOFCs using conventional extrusion	28
2.2	Recent development of single and multiple layer micro-tubular SOFCs using phase-inversion based extrusion	59
2.3	Comparison between Ram Extrusion and Phase Inversion-based Co-extrusion	64
2.4	Sintering additive effectiveness comparison	67
3.1	Equipment for characterizations	76
3.2	List of materials	77
3.3	Suspension composition of mix particle size CGO	78
3.4	Dual-layer hollow fiber suspension compositions	83
3.5	Extrusion parameters of the fabricated dual-layer hollow fiber precursor	85
4.1	Surface area, pore volume and pore size of the mix particles size CGO	97
5.1	Shrinkage temperature of Li-CGO powders	116
5.2	Binding energies and atomic concentrations of XPS survey spectrum on Li-CGO surface	118
5.3	Surface area of Li-CGO at different calcination temperature	122
5.4	FT-IR absorption band for functional group of CGO, LiNO ₃ , and Li-CGO	124
5.5	Electrolyte Suspension Compositions	126

6.1	Extrusion parameters of the fabricated NiO-CGO/Li-CGO precursor	135
7.1	Comparison of anode-supported micro-tubular SOFCs performance at 500 to 600 °C	163

LIST OF FIGURES

FIGURE NO.	TITLE	PAGE
1.1	Typical SOFC Designs	3
1.2	(A) The number of articles on micro-tubular SOFCs. The data is based on the number of articles mentioning micro-tubular SOFCs in the citation database Scopus in August 2016. (B) The country-wise distribution in micro-tubular SOFC research. The data is based on the number of articles mentioning micro-tubular SOFC in the citation database Scopus in August 2016	4
1.3	Geometries of SOFC [8]	5
1.4	Overall Thesis Structure	13
2.1	A generalized flow sheet for preparation of tubular SOFC [42]	16
2.2	Light optical photos of the YSZ electrolyte surfaces (a–c) during drying and (d) after sintering [9]	18
2.3	Photographs of C-shaped plastic tube holders [43]	19
2.4	Plastic mass ram extrusion process (Reproduced from [16])	20
2.5	Cross-sectional SEM images of the 0.8 mm tube after sintering at 1450 °C for 6 h in air [16]	21
2.6	SEM images of the anode tubes before reduction (a) Cell A (b) Cell B [53]	22
2.7	Microstructure of the LSM-supported micro tubular cell [55]	24
2.8	Optical micrographs showing (A) the green filaments fabricated using various reduction orifices and (B) the fabricated tubes after co-sintering at 1350 °C for 3 hours [88]	33

2.9	Schematic ternary phase diagram of polymer/solvent/non-solvent during polymeric membrane formation [92]	34
2.10	Asymmetric structure of ceramic hollow fiber precursor [95]	36
2.11	SEM Images of the YSZ electrolyte membrane with asymmetric structure [99]	37
2.12	SEM micrographs of the highly asymmetric YSZ hollow fiber precursors: (a) cross-sectional; (b) membrane wall [100]	38
2.13	Photo images of the (a) spinneret, (b) internal structure, and (c) examples of sintered NiO/YSZ hollow fibers [105]	40
2.14	Schematic of simulated current collecting modes for the hollow fiber micro-tubular SOFC. Case 1: (A) connections at same end; Case 2: (B) connections at both ends; Case 3: (C) connections at opposite ends; Case 4: (D) cathode 'mesh' connection along its length and anode single end and Case 5: (E) both cathode and anode meshes (ideal case) [107]	43
2.15	Schematic diagram of the phase inversion-based co-extrusion process of the dual-layer hollow fibers precursor [8]	47
2.16	Design and dimensions of the triple orifice spinneret [8]	47
2.17	SEM images of the (a) overall view and (b) cross-sectional view of the first generation dual-layer hollow fiber, co-sintered at 1500 °C [115]	48
2.18	SEM images of the second generation dual-layer hollow fibers [17]	50
2.19	SEM images of the third generation dual-layer hollow fibers [18]	51
2.20	Schematic diagram of the phase-inversion based co-extrusion process. The inset shows the picture of the quadruple-orifice spinneret (Data from [118])	54
2.21	SEM images (backscattered electrons (BSE) mode) of (a) whole view, (b) cross-section and (c) a higher magnification of cross-section of the sintered triple-layer hollow fibres, using the AFL extrusion rate at 3 ml/min (Data from [118])	54

2.22	SEM images of the fiber with the AFL extrusion rate of 2 ml min^{-1} : (a) overall view, (b) cross-section, (c) electrolyte/electrode interface [119]	55
2.23	Photographic pictures of (a) quadruple-orifice spinneret; (b) example of triple-layer precursors [119]	55
2.24	The Void at A Three Disk Junction which is Just Filled by a Touching Disk of Radius R_4 [42]	64
2.25	The Reduction in Specific Volume for Mixed Large and Small Spheres, showing the Condition of Optimal Packing where the Small Spheres fill all Voids in the Large Sphere Packing [42]	65
3.1	Research Methodology Flowchart	75
3.2	Steps involved in metal nitrate doping procedure	79
3.3	Fabrication procedure of flat sheet membrane precursor via phase inversion technique	80
3.4	Dual-layer hollow fiber fabrication steps	84
3.5	Structural design of a dual-layer hollow fiber	81
3.6	Schematic representation of three-point bending strength testing apparatus	87
3.7	Schematic diagram of apparatus for measuring gas permeation [8]	88
3.8	Set-up of two-point DC technique	89
3.9	Development of complete micro-tubular SOFC system	91
3.10	Schematic diagram of the micro-tubular SOFC performance test set-up	92
4.1	(a) Sintering curves and (b) sintering rate curves of electrolyte materials (heating rate $10 \text{ }^\circ\text{C min}^{-1}$)	94
4.2	Particle rearrangements during sintering (a) micron size, (b) mix particle size, (c) particle necking stage	95
4.3	N_2 adsorption-desorption isotherms and inset correspond to the BJH pore size distribution of electrolyte powders (a) N-00, (b) N-10, (c) N-20, (d) N-30, (e) N4-0 and (f) N-50	98
4.4	Viscosity data of the prepared suspensions	99
4.5	SEM cross sections images of N-30 and N-00 flat sheet electrolytes at different sintering temperatures	101

4.6	AFM images of N-30 at different sintering temperature: (a) 1350 (b) 1400 (c) 1450 ; (i) 3D view, (ii) height view, and (iii) lateral size distribution	103
4.7	Bending strength of the flat sheet at different sintering temperatures	104
4.8	Cross-section SEM images of the Ni–CGO/CGO N-00 and N-30 dual-layer hollow fiber at different co-sintering temperatures	106
4.9	Outer surface SEM images of the Ni–CGO/CGO N-00 and N-30 dual-layer hollow fiber at different co-sintering temperatures	107
4.10	Bending strength of the dual-layer hollow fiber at different co-sintering temperatures	108
4.11	Gas-tightness test result of the dual-layer hollow fibers at different co-sintering temperatures	109
5.1	TG and DSC curves of LiNO ₃	112
5.2	DSC of Li-CGO at different calcination temperature	113
5.3	TGA diagrams of LiNO ₃ , CGO and Li-CGO at different calcination temperature	114
5.4	(a) Sintering curves and (b) sintering rate curves of undoped CGO and Li doped CGO (heating rate 10 °C min ⁻¹)	115
5.5	TEM image and HRTEM image (a) as-prepared Li-CGO powder and (b) Li-CGO calcined at 700 °C	117
5.6	XPS spectrum of Li doped CGO electrolyte precursor	120
5.7	X-ray diffractograms of Li-CGO powders compared with LiNO ₃ and CGO	121
5.8	FT-IR spectrum of LiNO ₃ , CGO and Li-CGO powders at different calcination temperature	123
5.9	(a) D-140 and (b) D-500 flat sheets while immersing in water	127
5.10	SEM images of the full cross-section of the flat sheet	128
5.11	SEM cross sectional images of undoped CGO and Li-CGO at different sintering temperatures	129
5.12	SEM surface images of undoped CGO and Li-CGO at different sintering temperatures	130

5.13	Liquid Phase Sintering	132
5.14	X-ray diffractograms of D-700 flat sheet sintered at 1400 °C compared with D-700 and CGO	133
6.1	Microstructure of the dual-layer hollow fiber precursors	137
6.2	Photograph of Li-CGO dual-layer hollow fiber after sintering step; (a) 1350 °C (b)1400 °C (c) 1450 °C and (d) 1500 °C	138
6.3	Photograph of Li-CGO dual-layer hollow fiber after reducing step; (a) 1350 °C (b)1400 °C (c) 1450 °C and (d) 1500 °C	139
6.4	SEM images of the Li-CGO/Ni-CGO dual-layer hollow fiber at different co-sintering temperature: (a) 1450 °C, (b) 1500 °C, at different views. (1) Overall view of the hollow fiber, (2) cross-section of the hollow fiber, (3) anode cross-section of the hollow fiber, (4) electrolyte cross-section of the hollow fiber, (5) inner surface of the hollow fiber, (6) outer surface of the hollow fiber	141
6.5	Bending strength of the Li-CGO dual-layer hollow fibers at different co-sintering temperature	143
6.6	Cross-section SEM image of Ni-CGO/unmodified CGO co-sintered at 1450 °C	143
6.7	Gas-tightness property as a function of co-sintering temperature	144
7.1	Pore size distributions for the Ni–CGO hollow fiber at different sintering temperature	148
7.2	Porosity of the Ni–CGO anode hollow fibres as a function of sintering temperature	149
7.3	Triple-phase boundary (TPB) in Ni-CGO anode	150
7.4	The N ₂ permeation result of the Ni–CGO anode hollow fibres at different sintering temperature	151
7.5	Bending strength of the Ni–CGO anode hollow fibres at different sintering temperatures	152
7.6	Current-voltage characteristics at different sintering temperatures	153
7.7	Electrical conductivity of the anode layer hollow fibers	154

7.8	Cross-section SEM images of the dual-layer hollow fiber along with the zoomed outer layer which co-sintered at 1450 °C (a) unmodified CGO, (b) 30% nano-70% mic and (c) Li doped CGO	155
7.9	Bending strength and gas tightness properties of the dual-layer hollow fibers co-sintered at 1450 °C	158
7.10	Open-circuit voltage (OCV) and power density curves for modified CGO and unmodified CGO micro-tubular SOFCs at 500 °C with H ₂ fuel flow rate of 20 cm ³ min ⁻¹	160
7.11	Impedance spectra for modified CGO and unmodified CGO micro-tubular SOFCs measured at 500 °C	162

LIST OF ABBREVIATIONS

AFC	-	Alkaline fuel cell
ASTM	-	American Society for Testing and Materials
CaO	-	Calcium oxide
CO ₂	-	Carbon dioxide
CGO	-	Cerium gadolinium oxide
DMFC	-	Direct methanol fuel cell
DMSO	-	Dimethyl sulfoxide
Fe ₃ O ₄	-	Ferum oxide
H ₂	-	Hydrogen
H ₂ O	-	Water
HF	-	Hollow fibre
HT	-	High temperature
IT	-	Intermediate temperature
K ₂ CO ₃	-	Potassium carbonate
KOH	-	Potassium hydroxide
Li ₂ O	-	Lithium oxide
Li ₂ CO ₃	-	Lithium carbonate
LaMnO ₃	-	Lanthanum manganite
LSCF	-	Lanthanum strontium cobalt ferrite
LSM	-	Lanthanum strontium manganite
MCFC	-	Molten carbonate fuel cell
MgO	-	Magnesium Oxide
MIEC	-	Mixed ionic electron conductor
MT	-	Micro-tubular
Na ₂ CO ₃	-	Sodium carbonate
Ni	-	Nickel
NiO	-	Nickel oxide

NMP	-	N-methyl-2-pyrrolidinone
O ₂	-	Oxygen
OCV	-	Open circuit voltage
PAFC	-	Phosphoric fuel cell
PEMFC	-	Proton exchange membrane fuel cell
PES	-	Polyethersulfone
PF	-	Pore former
PMMA	-	Poly methyl methacrylate beads
RedOx	-	Reduced and Oxidation Atmosphere
Sc ₂ O ₃	-	Scandia Oxide
SEM	-	Scanning electron microscopy
SOFC	-	Solid oxide fuel cell
SSR	-	Sintering shrinkage rate
TEC	-	Thermal expansion coefficient
TGA	-	Thermo-gravimetric analysis
TPB	-	Triple-phase boundaries
XRD	-	X-ray diffraction
Y ₂ O ₃	-	Yttria oxide
YSZ	-	Yttria-stabilized zirconia
ZrO ₂	-	Zirconia oxide

LIST OF SYMBOLS

A	-	Area of hollow fibre
b	-	Width
B_F	-	Bending strength
cm	-	Centimetre
cP	-	Centipoise
D	-	Dry weight
d	-	Thickness
D_i	-	Inner diameter
D_o	-	Outer diameter
g	-	Gram
J	-	Joule
K	-	Kelvin
L	-	Length
L	-	Length of hollow fibre
m	-	Metre
min	-	Minute
mol	-	Mole
N	-	Load
nm	-	Nanometre
M	-	Saturated weight
P	-	Gas permeability
p_a	-	Atmospheric pressure
Pa	-	Pascal
p_o	-	Initial pressure
p_t	-	Final pressures
R	-	Gas constant
s	-	Second

<i>S</i>	-	Suspended weight
<i>T</i>	-	Temperature
<i>t</i>	-	Time for measurements
<i>V</i>	-	Voltage
<i>V_c</i>	-	Volume of the test cylinder
<i>W</i>	-	Watt
<i>wt</i>	-	Weight
°C	-	Degree Celsius
%	-	Percent
μm	-	Micrometre

LIST OF APPENDICES

APPENDIX	TITLE	PAGE
A	List of Publications	194
B	Sintering Additive Calculation	197

CHAPTER 1

INTRODUCTION

1.1 Research Background

Currently, the world is still dependent on fossil fuels as its major energy source. Nevertheless, the world today confronted with the issues of concern such as increasing energy consumption, energy security concerns, global warming and acid rain. Thus, using renewable energy and developing more efficient energy conversion devices have emerged as significant research and development (R&D) trends. Fuel cell is one of energy-conversion device that converts chemical energy directly to the electrical energy via electrochemical process. Hydrogen is the most common fuel, but hydrocarbons such as natural gas and alcohols like methanol are sometimes used. Unlike batteries, fuel cells need a constant source of fuel and oxygen/air to sustain the chemical reaction. Thus, as long as the input is supplied, fuel cells can produce electricity continuously.

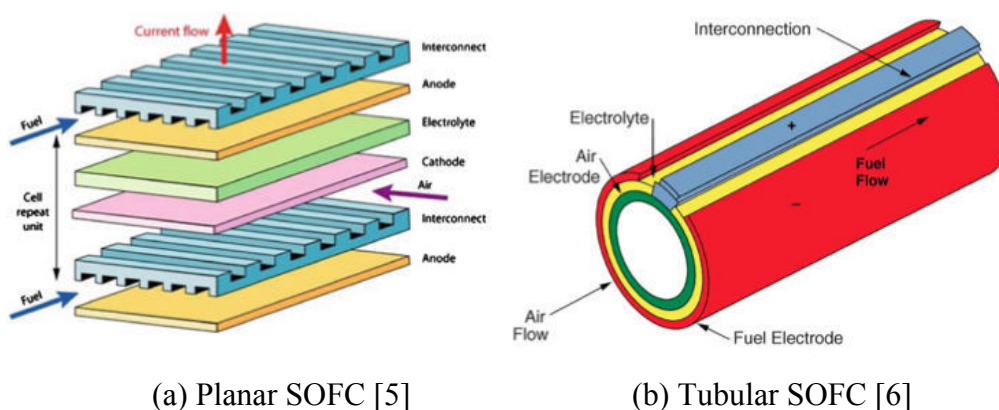
There are six common types of fuel cells as shown in Table 1.1. Primarily, their electrolyte classifies the fuel cells. This classification determines the chemical reactions that take place in the cell, the catalysts required, the temperature range in which the cell operates and the fuel required. These features typically affect the applications for which these cells are most suitable. In recent years, solid oxide fuel cells (SOFCs) have received tremendous attention due to their high-energy conversion efficiency, low emissions and excellent fuel flexibility.

Table 1.1 : Fuel Cell Types (U.S Department of Energy) [1]

Name	Electrolyte	Anode gas (fuel)	Cathode gas (oxidant)	Operating temperature	Development Status
AFC (Alkaline Fuel Cell)	Potash	Hydrogen	Oxygen	Below 80 °C	Commercial
PEMFC (Proton Exchange Membrane Fuel Cell)	Polymer Membrane	Hydrogen	Oxygen or Atmospheric Oxygen	to 120 °C	Being developed
DMFC (Direct Methanol Fuel Cell)	Polymer Membrane	Methanol	Atmospheric Oxygen	90 – 120 °C	Being developed
PAFC (Phosphoric Acid Fuel Cell)	Phosphorus	Hydrogen	Atmospheric Oxygen	200 °C	Commercial
MCFC (Molten Carbonated Fuel Cell)	Alkali-carbonates	Hydrogen Methane	Atmospheric Oxygen	650 °C	Being developed
SOFC (Solid Oxide Fuel Cell)	Ceramic Oxide	Hydrogen Methane	Atmospheric Oxygen	500 – 1000 °C	Being developed

Since 1960s, many studies conducted on solid oxide fuel cells (SOFCs) have been focusing on compact design and cell performance enhancement. Most of the developments focus on planar and tubular designs as shown in Figure 1.1. Typically, fabrication of planar SOFCs is cheaper due to its simpler techniques such as tape

casting and screen printing [2]. Furthermore, the planar SOFCs offer higher power densities production due to inherently shorter path lengths for electrons to travel from anode to cathode sides. However, the design has certain disadvantages including inherently lower thermal stability and larger areas that require high temperature for gas sealing. On the other hand, the tubular type is relatively well-established in terms of design and manufacturing technology [3]. It offers better thermo-cycling behavior and easier sealing around the circumference of the tubes [4]. However, its difficulty in designing complete interconnects axially and circumferentially because it creates longer current paths which often increase the ohmic loss. It also decreases the power densities as compared with its planar counterpart.



(a) Planar SOFC [5]

(b) Tubular SOFC [6]

Figure 1.1 Typical SOFC Designs

Started in early 1990s, Kendall and co-workers initiated an advanced cell design namely micro-tubular SOFCs [2]. This invention was driven from the effort to improve the performance of tubular SOFCs by reducing the cell size, from centimeter to the micron scale. It is remarkable that various potential benefits appear when the diameter gets smaller. The micro-tubular SOFC offers a greater tolerance to thermal cycling, quicker start-up capability, higher volumetric output density and portable characteristics compared to the conventional planar and tubular SOFCs [7]. These characters have promoted the research in micro-tubular SOFCs. Figure 1.2 (A) shows the analyze result from ‘Scopus’ search which reveals the increase in the number of articles published on micro-tubular SOFC over the last one decade (2006–2016). Besides, the reported electric current output from the micro-tubular SOFCs

has also increased greatly over the recent years. Figure 1.2 (B) shows the country-wise distribution of micro-tubular SOFC researchers, the data that was also drawn from ‘Scopus’. It is noticeable that the attraction in micro-tubular SOFC research is worldwide with increasing number of researchers from different countries.

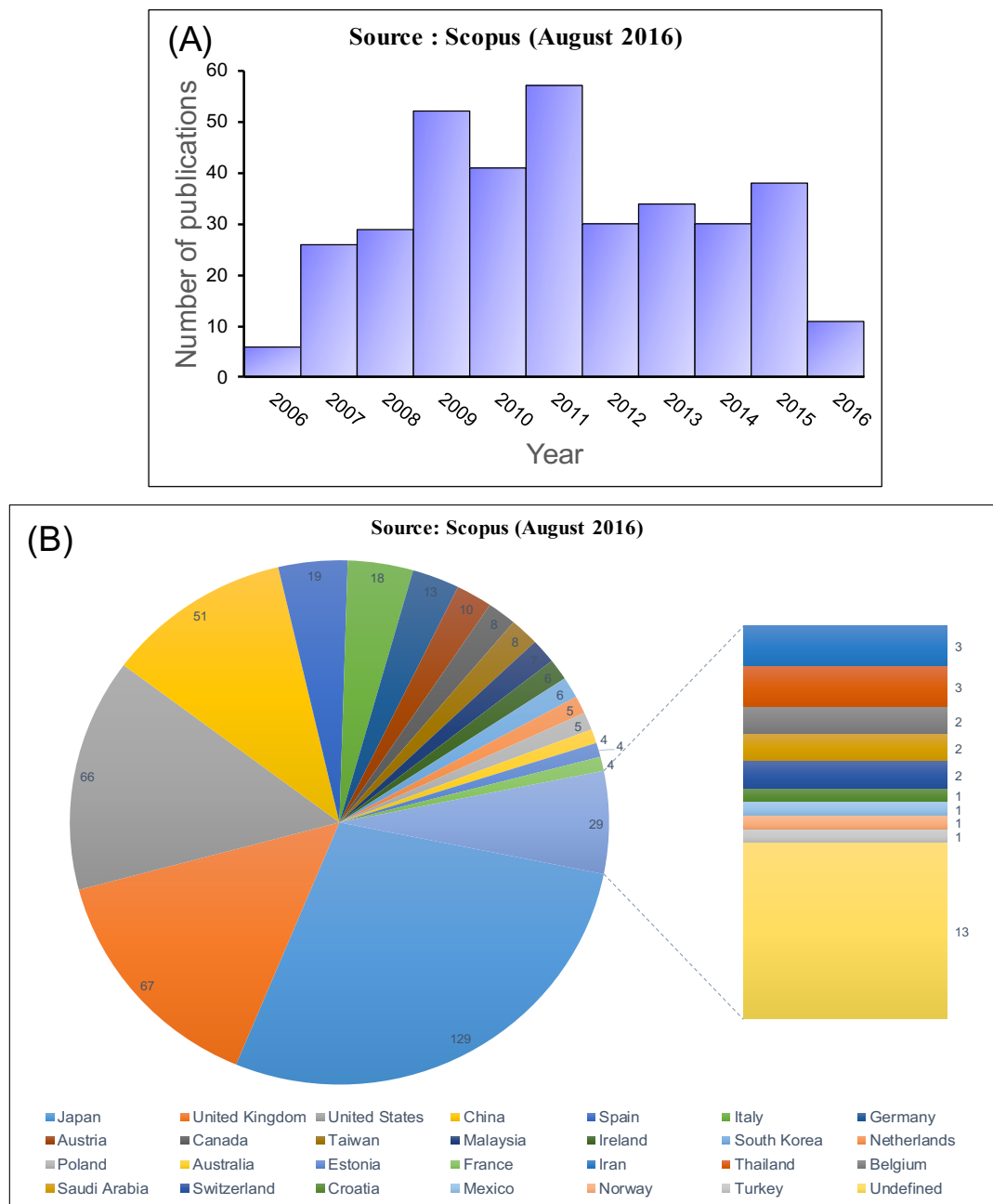


Figure 1.2 (A) The number of articles on micro-tubular SOFCs. The data is based on the number of articles mentioning micro-tubular SOFCs in the citation database Scopus in August 2016. (B) The country-wise distribution in micro-tubular SOFC research. The data is based on the number of articles mentioning micro-tubular SOFC in the citation database Scopus in August 2016.

Generally, the design of SOFC can be configured into two geometries; self-supporting and supported concept [8]. As depicted in Figure 1.3, self-supporting refers to the electrolyte with thickness around 80-250 μm forms as structural element of the design while for the supported concept, the electrolyte is deposited as a thin layer $<50 \mu\text{m}$ on porous electrode either cathode or anode.

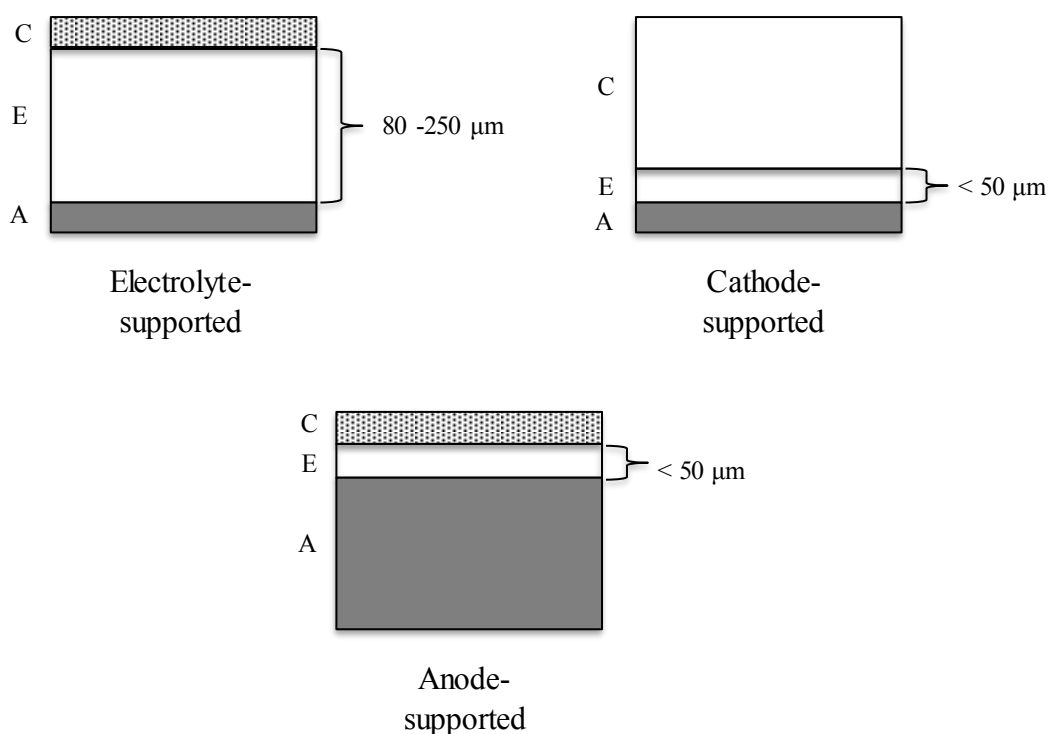


Figure 1.3 Geometries of SOFC [9]

The micro-tubular SOFCs can be constructed into the anode supported, the cathode supported or the electrolyte supported configurations depending on the component providing the mechanical strength to the micro-tubular cells. The use of anode-supported design allows for a thinner electrolyte layer, which reduces electrolytic resistance losses and yields better conductance at lower temperatures compared to an electrolyte supported [10]. This configuration is generally recognized to increase the performance, but additional caution is needed to avoid the formation of microcracks and to ensure the electrolyte layer is entirely gas tight. Nevertheless, it should be addressed that majority of recent works on micro-tubular SOFCs uses the anode-supported design.

Recently, there is a trend to move to lower temperature operation, which is intermediate (500-700 °C) or low (<500 °C) operating temperature. High operating temperature system possesses several disadvantages on commercialization for instance, long-term stability of the cell components, materials as well as high manufacturing cost. Moreover, high operating temperature limits the range of material selection. In comparison to lower temperature operation, it affords more rapid start-up, improved durability, and higher robustness as well as simplified system requirements and wider choice of selecting materials.

Consequently, the electrolytes with high oxygen-ion conductivity at low temperatures have received tremendous attractions. Cerium gadolinium oxide (CGO) is an attractive electrolyte alternative to yttria stabilized zirconia (YSZ), owing to its superior oxygen ion conductivity at low temperatures [11]. Like zirconia, ceria-based electrolytes have a cubic, fluorite-type crystal structure. This structure affords the large oxygen ions with high mobility. However, at low oxygen partial pressures and at higher temperatures ceria is partially reduced and the material becomes an electronic conductor, which can cause short circuit [12]. Although the stability of ceria in low oxygen partial pressures is inferior to that of zirconia, the chemical stability of ceria with cathode materials is superior to that of zirconia. CGO has been shown to be stable with a wide variety of electrodes, including lanthanum strontium manganate (LSM), lanthanum strontium cobalt (LSC), lanthanum strontium ferrite (LSF), lanthanum strontium cobalt ferrite (LSCF) and lanthanum nickel ferrite (LNF) [13].

Indeed, the general requirements for an electrolyte are high ionic conductivity, low electronic conductivity, and stable in both oxidizing and reducing environments with good mechanical properties [12–15]. Thus, the electrolyte structure must be dense because it acts as membrane that separates the air and fuel compartments and must be an oxygen ion conductor. Henceforth, electrolyte is the heart of the fuel cell whereby it determines the performance of the cell. Literature studies shows that two electrolyte systems specifically YSZ and CGO have been widely explored for SOFCs [13][15]. Each electrolyte system offers advantages

along with a number of drawbacks. Table 1.2 shows the general comparison between YSZ and CGO systems.

Table 1.2 : Comparison between YSZ and CGO systems

Electrolyte system	YSZ	CGO
Operating Temp	High Temp (800 – 1000 °C)	Intermediate Temp (500-700 °C)
Material Cost	Relatively less expensive	Relatively expensive
TEC	$10.5 \times 10^{-6} \text{ K}^{-1}$	$12.5 \times 10^{-6} \text{ K}^{-1}$
Conductivity	Ionic conductivity	Mixed ionic electronic conductivity at high temperature and low oxygen partial pressure
Mechanical strength	Sufficient mechanical strength	Ceria electrolytes are unstable mechanically at temperatures above 700 °C
Reaction with electrodes material	Chemical reaction with the cathode material	Unreactive towards potential electrode materials
Advantages	Provide high quality exhaust heat for cogeneration, and when pressurized, can be integrated with a gas turbine to further increase the overall efficiency of the power system.	Improved durability, wider choice for interconnecting material selection, and lower costs can be achieved by reducing the operating temperature below 700 °C

As shown in Table 1.2, YSZ fulfills the electrical requirements at high temperatures (800 - 1000 °C) and has good high temperature mechanical properties. However, one of its drawbacks is its reactivity with perovskite oxide electrodes such as LSM. At high temperatures, they react and forming pyrochlore, $\text{La}_2\text{Zr}_2\text{O}_7$, the perovskite SrZrO_3 or both [12]. Unless, the YSZ layer is protected with CGO layer [15]. Alternatively, CGO has received great attention as an electrolyte material and

it has the highest conductivity at lower temperature and lower polarization resistance [34]. Besides, doped ceria is more stable and relatively unreactive towards potential electrode materials.

Besides the progress in SOFC designs, development in the fabrication process is critically important to ensure the success of the cell. Previously, the fabrication of micro-tubular SOFC, which consists of three main components (i.e. anode, electrolyte and cathode), can only be achieved through multiple steps [17]. There are two common techniques that have been employed to fabricate the support of the cell which are plastic mass ram extrusion and dry-jet wet extrusion. For the ram extrusion technique, the support materials are mixed with binder and solvent to form a viscous paste. The paste is then extruded through a custom-made die using a ram extruder to obtain the support tubes. The support tubes are dried and cut to the desired length prior being subjected to the sintering process. The fabricated support tubes are usually of a symmetrical structure with large wall thicknesses, which results in a large resistance for the diffusion of fuel into the anode (in the case of anode-supported design).

In contrast, the dry-jet wet extrusion technique offers greater control over the morphology of hollow fiber (common terminology for the tubes prepared using this technique). The dry-jet wet extrusion is similar to the ram extrusion process. The main difference is that the spinning suspension or dope for the dry-jet wet extrusion is in suspension form and the ram extrusion is in paste or plastic mass form. Another major difference is the solidification process of the tube (or hollow fiber). In dry-jet wet extrusion, the solidification of the hollow fiber occurs via phase inversion process initiated by the solvent/non-solvent exchange. While in ram extrusion process, the tube is dried straight away after the extrusion prior to being subjected to the sintering process.

However, both techniques are only used to fabricate a single-layer of support, and thus, still require a multi-step in order to develop a complete fuel cell. By using dry-jet wet or ram extrusions, a support layer for example anode tube is first prepared and pre-sintered to provide mechanical strength to the fuel cell. The

electrolyte layer is then deposited and sintered prior to the final coating of cathode layer. Each step involves at least one high temperature heat treatment, making the cell fabrication time-consuming and costly with unstable control over cell quality.

For a more economical fabrication of micro-tubular SOFC with reliability and flexibility in quality control, an advanced dry-jet wet extrusion technique, i.e. a phase inversion-based co-extrusion process, is recently employed to fabricate a dual-layer hollow fiber, which consists of electrolyte and anode for intermediate temperature SOFC (IT-SOFC)[18]. Co-extrusion technique in developing an electrolyte/anode dual-layer hollow fiber for micro-tubular SOFC pioneered by Li and co-workers [19] and the cell from the prepared hollow fiber showed a very outstanding power output, approximately 2.32 Wcm^{-2} , which is almost double than the one prepared from conventional multi-step technique [20][21]. In comparison with conventional extrusion processes, the co-extrusion is more attractive due to the following reasons: (i) saving the production cost and time as it combines a number of processes into one; (ii) decreasing the risk of inducing defect; (iii) producing a great adhesion between layers.

1.2 Problem Statement

To date, IT-SOFC is more promising compared to HT-SOFC ones due to their better long-term durability and cost effectiveness. It has been reported that CGO possesses 4 to 5 times higher conductivity at lower operating temperatures [22–28], and thus, make it more suitable to be used as the electrolyte for IT-SOFC. However, sintering temperatures as high as $1550 \text{ }^{\circ}\text{C}$ are typically needed to densify CGO electrolyte [29] which increasing cost and difficulty in the cell fabrication process. Moreover, sintering of the layers at too high temperatures to obtain full densification of the electrolyte layer would cause an interfacial interdiffusion between the electrolyte and electrodes material which eventually generate a highly resistive interface that can diminish the ionic conductivity [30]. It should be note that high sintering temperature might reduce the porosity in the electrodes layers as well [31] particularly in the co-sintering step [18] of dual-layer hollow fiber (HF).

Keeping in mind that the anode component; usually nickel oxide (NiO), are normally sintered at 1400 °C, steps would be taken to lower the sintering temperature of electrolyte material so that it can be co-sintered together with the anode at lower temperature. Thus, modification of the electrolyte sintering properties is needed to establish an appropriate sintering profile that allows the production defect-free micro-tubular SOFC hollow fiber precursor with the desired microstructure and low energy consumption.

Currently, it has been reported that introducing metal oxides as the sintering additive can effectively reduce the sintering temperature of CGO up to 900-1200 °C [32–34] by liquid phase sintering mechanism. On the other hand, successful attempts of CGO sintered at 1250 - 1400 °C has been reported by introducing nano size particle of CGO as the starting powder [35–40]. As the small particles size exhibiting as high driving force [41], it is hypothesized that nano size powders enhance the densification at lower temperature. Nevertheless, the previous works only reported on CGO button cells prepared by pressing method. To the best of author's knowledge, study on the effect of sintering additive and nano size particles on electrolytes densification prepared by phase inversion technique, has yet been reported. The feasibility of these approaches on phase inversion based co-extrusion/co-sintering technique is still unclear.

Realising the huge potential that is offered by phase inversion based co-extrusion/co-sintering technique, it is relevant to implement these two approaches in reducing the sintering temperature of CGO and understanding how it affects the microstructure, densification temperature, mechanical strength, gas tightness properties as well as the micro-tubular SOFC performance. This study is expected will produce a good quality micro-tubular SOFC with shorter fabrication time and thus the outcome is very novel and beneficial to the researchers in this area.

1.3 Objectives and Scopes

The main objective of this study is to develop anode/electrolyte dual-layer hollow fibres with improved electrolyte properties and reduced sintering temperature for intermediate temperature micro-tubular solid oxide fuel cells (SOFCs) via a single-step phase inversion-based co-extrusion/co-sintering technique. This objective has been achieved by accomplishing the following specific objectives:

- a) To design the experiment in modifying the sintering properties of CGO electrolyte flat sheet via two approaches i.e; mix particle size CGO and sintering additive.
- b) To fabricate an anode/electrolyte of both modified dual-layer hollow fiber solid oxide fuel cell by using a promising phase inversion-based co-extrusion/co-sintering technique.
- c) To study the properties of both modified dual-layer hollow fiber in terms of its morphology, conductivity, electrolyte tightness, anode permeability and mechanical strength.
- d) To conduct the current-voltage performance of both modified dual-layer hollow fiber as a complete SOFC.

In order to achieve the objectives, four scopes have been identified in this research. The scopes are:

- a) Modifying the sintering properties of electrolyte via two approaches.
- b) Fabricating anode/electrolyte of both modified dual-layer hollow fiber via co-extrusion/co-sintering technique.
- c) Characterizing the physical and chemical properties of both modified dual-layer hollow fiber in terms of its morphology, crystal structure, mechanical strength, gas-tightness properties and gas permeability.
- d) Performing micro-tubular SOFC test by potentiostat/galvanostat at temperature 500 °C.

1.4 Significance of Study

This study is expected to provide a better understanding on the fundamental principle for the fabrication of dual-layer hollow fiber for micro-tubular SOFC, which consists of the modifications of electrolyte layer by considering the morphological, mechanical strength and gas tightness of the precursors. It is acknowledged that nano size particles and sintering additive has been used in various fabrication techniques to reduce the sintering temperature of CGO, however little attention has been given on their application in phase-inversion technique. Therefore, attempts are made to investigate the potential of nano size CGO and Li_2O as sintering additive in this technique. By identifying the ideal characteristics of the nano size loadings and behaviors of the sintering additive, high performance micro-tubular SOFCs can be fabricated.

Up to now, no study has been conducted to implement these two approaches in preparing dual-layer hollow fiber via phase-inversion technique. This study could be beneficial to the researchers in this area regarding to the knowledge generation on fabricating modified dual-layer hollow fiber using a single-step technique. In addition, with the utilization of low sintered electrolyte, an improved quality of SOFCs component can be produced. This study has proven the possibility to accelerate the densification by incorporating nano size CGO and sintering additives as well as presented an advanced new material to reduce the sintering temperature of CGO. Thus, it would lead to the development of low cost micro-tubular solid oxide fuel cell, in order to make fuel cell technology able to compete economically with traditional energy technologies.

1.5 Thesis Organisation

This thesis consists of 8 Chapters and its organization is shown in Figure 1.4. Chapter 1 briefly introduces the research background of fuel cells particularly the micro tubular solid oxide fuel cell, the objectives and scopes of the study and overview of the thesis. Chapter 2 describes the literature review on conventional and

recent introduced phase inversion-based extrusion techniques, their characteristics and performances. It also provides a review on recent approaches to reduce the densification temperature of CGO. Other than that, the future direction is presented as well. Chapter 3 presents a detailed methodology of this research work in order to achieve the targeted objectives.

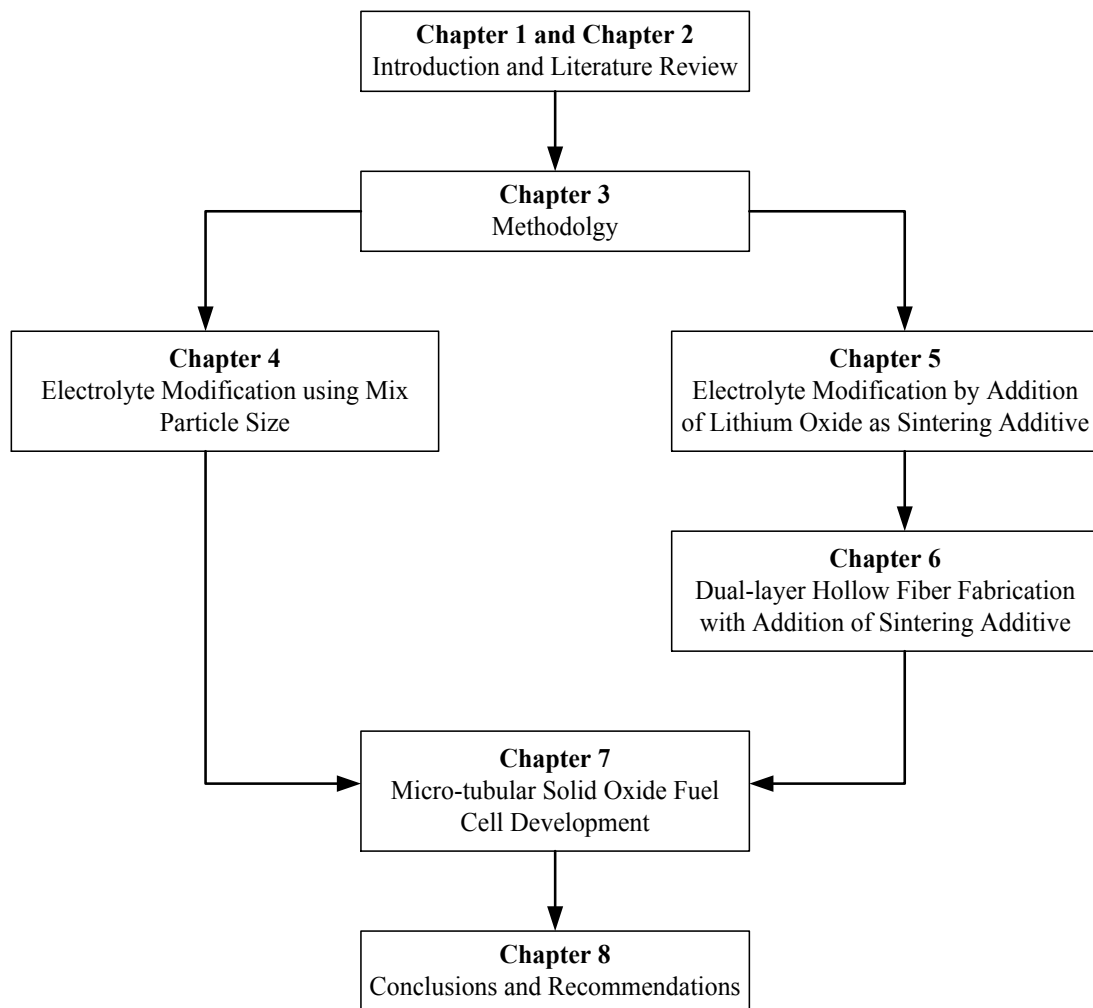


Figure 1.4 Overall Thesis Structure

Chapter 4 reports the potential of the first approach which is introducing mix particle size of CGO to reduce the densification temperature. The first part focuses on the particles behavior particularly the shrinkage rate of the mix particle size CGO. The second part clarifies the effect of nano size loading to the characteristics of the dope suspension and flat sheet. While the last part reports the development of dual-layer hollow fibers using the modified electrolyte. This includes the study on the

REFERENCES

1. U.S Department of Energy, *Comparison of Fuel Cell Technologies*, Available from: <http://energy.gov/eere/fuelcells/downloads/comparison-fuel-cell-technologies-fact-sheet>. 2016.
2. Singhal, S. C. and Kendall, K. *High Temperature Solid Oxide Fuel Cells*, Subhash C. Singhal and Kevin Kendal, Eds. UK: Elsevier Advanced Technology. 2003.
3. Sammes, N. M., Du, Y. and Bove, R. Design and fabrication of a 100W anode supported micro-tubular SOFC stack. *J. Power Sources*, 2005, 145 (2): 428–434.
4. Akkaya, A. V. Electrochemical model for performance analysis of a tubular SOFC. *Int. J. Energy Res.*, 2007, 31: 79–98.
5. Zuo, C., Liu, M. and Liu, M. Solid Oxide Fuel Cells. In: Sol-Gel Processing for Conventional and Alternative Energy. In, Aparicio, M., Jitianu, A., Klein, L. C., Eds., Springer: New York, 2012.
6. Williams, M. C., Strakey, J. P. and Singhal, S. C. U.S. distributed generation fuel cell program. *J. Power Sources* 2004, 131 (1-2): 79–85.
7. Meng, X., Gong, X., Yang, N., Tan, X., Yin, Y. and Ma, Z. F. Fabrication of Y_2O_3 -stabilized- ZrO_2 (YSZ)/ $La_{0.8}Sr_{0.2}MnO_{3-\alpha}$ -YSZ dual-layer hollow fibers for the cathode-supported micro-tubular solid oxide fuel cells by a co-spinning/co-sintering technique. *J. Power Sources* 2013, 237: 277–284.
8. Badwal, S. P. S. and Foger, K. Solid Oxide Electrolyte Fuel Cell Review. 1996, 8842 (95): 257–265.
9. Othman, M. H. D. *High performance micro-tubular solid oxide fuel cell*. Ph.D thesis, Imperial College, 2011.
10. Du, Y. and Sammes, N. M. Fabrication and properties of anode-supported tubular solid oxide fuel cells. *J. Power Sources* 2004, 136(1): 66–71.

11. Lawlor, V., Griesser, S., Buchinger, G., Olabi, A. G., Cordiner, S. and Meissner, D. Review of the micro-tubular solid oxide fuel cell. *J. Power Sources* 2009, 193(2): 387–399.
12. Fergus, J. W. Electrolytes for solid oxide fuel cells. *J. Power Sources* 2006, 162(1): 30–40.
13. Wincewicz, K. C. and Cooper, J. S. Taxonomies of SOFC material and manufacturing alternatives. *J. Power Sources* 2005, 140(2): 280–296.
14. Veranitisagul, C., Kaewvilai, A., Wattanathana, W., Koonsaeng, N., Traversa, E. and Laobuthee, A. Electrolyte materials for solid oxide fuel cells derived from metal complexes: Gadolinia-doped ceria. *Ceram. Int.* 2012, 38,(3): 2403–2409.
15. Antoni, L. Materials for Solid Oxide Fuel Cells: The Challenge of Their Stability. *Mater. Sci. Forum* 2004, 461-464: 1073–1090.
16. Lawlor, V. Review of the micro-tubular solid oxide fuel cell (Part II: Cell design issues and research activities). *J. Power Sources* 2013, 240: 421–441.
17. Suzuki, T., Yamaguchi, T., Fujishiro, Y. and Awano, M. Fabrication and characterization of micro tubular SOFCs for operation in the intermediate temperature. *J. Power Sources* 2006, 160(1): 73–77.
18. Othman, M. H. D., Wu, Z., Droushiotis, N., Doraswami, U., Kelsall, G. and Li, K. Single-step fabrication and characterisations of electrolyte/anode dual-layer hollow fibres for micro-tubular solid oxide fuel cells. *J. Memb. Sci.* 2010, 351(1-2): 196–204.
19. Othman, M. H. D., Droushiotis, N., Wu, Z., Kelsall, G. and Li, K. Dual-layer hollow fibres with different anode structures for micro-tubular solid oxide fuel cells. *J. Power Sources* 2012, 205: 272–280.
20. Suzuki, T., Hasan, Z., Funahashi, Y., Yamaguchi, T., Fujishiro, Y. and Awano, M. Impact of anode microstructure on solid oxide fuel cells. *Science* 2009, 325(5942): 852–855.
21. Sin, Y. W., Galloway, K., Roy, B., Sammes, N. M., Song, J.-H., Suzuki, T. and Awano, M. The properties and performance of micro-tubular (less than 2.0mm O.D.) anode supported solid oxide fuel cell (SOFC). *Int. J. Hydrogen Energy* 2011, 36(2): 1882–1889.

22. Kaiser, A., Prasad, A. S., Foghmoes, S. P., Ramousse, S., Bonanos, N. and Esposito, V. Sintering process optimization for multi-layer CGO membranes by in situ techniques. *J. Eur. Ceram. Soc.* 2013, 33(3): 549–556.
23. Chen, M., Hallstedt, B., Grundy, A. N. and Gauckler, L. J. CeO₂-CoO Phase Diagram. *J. Am. Ceram. Soc.* 2003, 86(9): 1567–1570.
24. Fagg, D. P., Kharton, V. V. and Frade, J. R. P-Type Electronic Transport in Ce_{0.8}Gd_{0.2}O_{2-δ}: The Effect of Transition Metal Oxide Sintering Aids. *J. Electroceramics* 2002, 9: 199–207.
25. Fagg, D. P., Abrantes, J. C. C., Pérez-Coll, D., Núñez, P., Kharton, V. V. and Frade, J. R. The effect of cobalt oxide sintering aid on electronic transport in Ce_{0.80}Gd_{0.20}O_{2-δ} electrolyte. *Electrochim. Acta* 2003, 48(8): 1023–1029.
26. Fagg, D. P., Kharton, V. and Frade, J. R. Transport in ceria electrolytes modified with sintering aids: effects on oxygen reduction kinetics. *J. Solid State Electrochem.* 2004, 8(9): 618–625.
27. Gil, V., Tartaj, J., Moure, C. and Durán, P. Sintering, microstructural development, and electrical properties of gadolinia-doped ceria electrolyte with bismuth oxide as a sintering aid. *J. Eur. Ceram. Soc.* 2006, 26(15): 3161–3171.
28. Zhang, L., Lan, R., Cowin, P. I. and Tao, S. Fabrication of solid oxide fuel cell based on doped ceria electrolyte by one-step sintering at 800°C. *Solid State Ionics* 2011, 203(1): 47–51.
29. Maca, K., Pouchly, V. and Zalud, P. Two-Step Sintering of oxide ceramics with various crystal structures. *J. Eur. Ceram. Soc.* 2010, 30(2): 583–589.
30. Kuo, Y. L. and Su, Y. M. Sintering behaviour and electrical properties of gadolinia-doped ceria modified by addition of silicon oxide and titanium oxide. *Micro Nano Lett.* 2012, 7(5): 472.
31. Zhao, L., Zhang, X., He, B., Liu, B. and Xia, C. Micro-tubular solid oxide fuel cells with graded anodes fabricated with a phase inversion method. *J. Power Sources* 2011, 196(3): 962–967.
32. Perezcoll, D., Nunez, P., Abrantes, J., Fagg, D., Kharton, V., Frade, J. Effects of firing conditions and addition of Co on bulk and grain boundary properties of CGO. *Solid State Ionics* 2005, 176(37-38): 2799–2805.
33. Han, M.-F., Zhou, S., Liu, Z., Lei, Z. and Kang, Z. C. Fabrication, sintering and electrical properties of cobalt oxide doped Gd_{0.1}Ce_{0.9}O_{2-δ}. *Solid State Ionics* 2011, 192(1): 181–184.

34. Le, S., Zhu, S., Zhu, X. and Sun, K. Densification of Sm_{0.2}Ce_{0.8}O_{1.9} with the addition of lithium oxide as sintering aid. *J. Power Sources* 2013, 222: 367–372.
35. Glasscock, J. A., Esposito, V., Foghmoes, S. P. V, Stegk, T., Matuschek, D., Ley, M. W. H. and Ramousse, S. The effect of forming stresses on the sintering of ultra-fine Ce_{0.9}Gd_{0.1}O_{2-δ} powders. *J. Eur. Ceram. Soc.* 2013, 33: 1289–1296.
36. Gil, V., Gurauskis, J., Campana, R., Merino, R. I., Larrea, A. and Orera, V. M. Anode-supported microtubular cells fabricated with gadolinia-doped ceria nanopowders. *J. Power Sources* 2011, 196(3): 1184–1190.
37. Muralidharan, P., Jo, S. H. and Kim, D. K. Electrical Conductivity of Submicrometer Gadolinia-Doped Ceria Sintered at 1000°C Using Precipitation-Synthesized Nanocrystalline Powders. *J. Am. Ceram. Soc.* 2008, 91(10): 3267–3274.
38. Jo, S. H., Muralidharan, P. and Kim, D. K. Electrical characterization of dense and porous nanocrystalline Gd-doped ceria electrolytes. *Solid State Ionics* 2008, 178(39-40): 1990–1997.
39. Ruiz-Trejo, E., Santoyo-Salazar, J., Vilchis-Morales, R., Benítez-Rico, A., Gómez-García, F., Flores-Morales, C., Chávez-Carvayar, J. and Tavizón, G. Microstructure and electrical transport in nano-grain sized Ce_{0.9}Gd_{0.1}O_{2-δ} ceramics. *J. Solid State Chem.* 2007, 180(11): 3093–3100.
40. Zhang, T. S., Ma, J., Kong, L. B., Chan, S. H., Kilner, J. A. Aging behavior and ionic conductivity of ceria-based ceramics: a comparative study. *Solid State Ionics* 2004, 170(3-4): 209–217.
41. Jud, E., Huwiler, C. B. and Gauckler, L. J. Sintering Analysis of Undoped and Cobalt Oxide Doped Ceria Solid Solutions. *J. Am. Ceram. Soc.* 2005, 88(11): 3013–3019.
42. George, R. A. Status of tubular SOFC field unit demonstrations. *J. Power Sources* 2000, 86: 134–139.
43. Li, K. *Ceramic Membranes for Separation and Reaction*, England: John Wiley & Sons Ltd. 2007.
44. Sammes, N. M. and Du, Y. Fabrication and Characterization of Tubular Solid Oxide Fuel Cells. *Int. J. Appl. Ceram. Technol.* 2007, 4(2): 89–102.

45. Garcia, R. D. T. Production of Micro-Tubular Solid Oxide Fuel Cells, Ph.D thesis, University of Trento, 2011.
46. Suzuki, T., Yamaguchi, T., Fujishiro, Y. and Awano, M. Improvement of SOFC performance using a microtubular, anode-supported SOFC. *J. Electrochem. Soc.* 2006, 153(5): A925–A928.
47. Yamaguchi, T., Suzuki, T., Shimizu, S., Fujishiro, Y. and Awano, M. Examination of wet coating and co-sintering technologies for micro-SOFCs fabrication. *J. Memb. Sci.* 2007, 300(1-2): 45–50.
48. Suzuki, T., Funahashi, Y., Yamaguchi, T., Fujishiro, Y. and Awano, M. Fabrication and characterization of micro tubular SOFCs for advanced ceramic reactors. *J. Alloys Compd.* 2008, 451(1-2): 632–635.
49. Suzuki, T., Funahashi, Y., Hasan, Z., Yamaguchi, T., Fujishiro, Y. and Awano, M. Fabrication of needle-type micro SOFCs for micro power devices. *Electrochem. commun.* 2008, 10: 1563–1566.
50. Funahashi, Y., Shimamori, T., Suzuki, T., Fujishiro, Y. and Awano, M. Fabrication and characterization of components for cube shaped micro tubular SOFC bundle. *J. Power Sources* 2007, 163(2): 731–736.
51. Suzuki, T., Yamaguchi, T., Fujishiro, Y. and Awano, M. Current collecting efficiency of micro tubular SOFCs. *J. Power Sources* 2007, 163(2): 737–742.
52. Suzuki, T., Funahashi, Y., Yamaguchi, T., Fujishiro, Y. and Awano, M. New Stack Design of Micro-tubular SOFCs for Portable Power Sources. *Fuel Cells* 2008, 8(6): 381–384.
53. Suzuki, T., Funahashi, Y., Yamaguchi, T., Fujishiro and Y., Awano, M. Design and fabrication of lightweight, submillimeter tubular solid oxide fuel cells. *Electrochem. solid-state Lett.* 2007, 10(8): A177–A179.
54. Suzuki, T., Funahashi, Y., Yamaguchi, T., Fujishiro, Y. and Awano, M. Effect of anode microstructure on the performance of micro tubular SOFCs. *Solid State Ionics* 2009, 180(6-8): 546–549.
55. Yamaguchi, T., Shimizu, S., Suzuki, T., Fujishiro, Y. and Awano, M. Fabrication and evaluation of cathode-supported small scale SOFCs. *Mater. Lett.* 2008, 62(10-11): 1518–1520.

56. Yamaguchi, T., Shimizu, S., Suzuki, T., Fujishiro, Y. and Awano, M. Fabrication and characterization of high performance cathode supported small-scale SOFC for intermediate temperature operation. *Electrochemistry Communications* 2008, 10(9): 1381–1383.
57. Liu, Y., Hashimoto, S.-I., Nishino, H., Takei, K., Mori, M., Suzuki, T. and Funahashi, Y. Fabrication and characterization of micro-tubular cathode-supported SOFC for intermediate temperature operation. *J. Power Sources* 2007, 174(1): 95–102.
58. Sammes, N. M., Song, J., Roy, B., Galloway, K., Suzuki, T., Awano, M. and Serincan, A. M. F. A Study of GDC-Based Micro Tubular SOFC. *Mater. Sci. Forum* 2010, 638-642: 1152–1157.
59. Suzuki, T., Funahashi, Y., Yamaguchi, T., Fujishiro, Y. and Awano, M. *Development of Fabrication/Integration Technology for Micro Tubular SOFCs*, Elsevier Inc. 2009.
60. Calise, F., Restuccia, G. and Sammes, N. Experimental analysis of micro-tubular solid oxide fuel cell fed by hydrogen. *J. Power Sources* 2010, 195(4): 1163–1170.
61. Hsieh, W.-S., Lin, P. and Wang, S.-F. Fabrication of electrolyte supported micro-tubular SOFCs using extrusion and dip-coating. *Int. J. Hydrogen Energy* 2013, 38(6): 2859–2867.
62. Schoonman, J., Dekker, J., Broers, J. and Kiwiet, N. Electrochemical vapor deposition of stabilized zirconia and interconnection materials for solid oxide fuel cells. *Solid State Ionics* 1991, 46(3-4): 299–308.
63. Cherng, J. S., Wu, C. C., Yu, F. A. and Yeh, T. H. Anode morphology and performance of micro-tubular solid oxide fuel cells made by aqueous electrophoretic deposition. *J. Power Sources* 2013, 232: 353–356.
64. Zhang, H., Rui, D., Zhang, K. and Wang, G. Fabrication of Solid Oxide Fuel Cells with Powder / Suspension Plasma Spraying. *Progress In Electromagnetics Research Symposium Proceedings August 18–21, 2009, Moscow, Russia: 2009.* 1965–1970.
65. Liu, Y., Mori, M., Funahashi, Y., Fujishiro, Y. and Hirano, A. Development of micro-tubular SOFCs with an improved performance via nano-Ag impregnation for intermediate temperature operation. *Electrochem. commun.* 2007, 9(8): 1918–1923.

66. Lee, T. J. and Kendall, K. Characterisation of electrical performance of anode supported micro-tubular solid oxide fuel cell with methane fuel. *J. Power Sources* 2008, 181(2): 195–198.
67. Akhtar, N., Decent, S. P., Loghin, D. and Kendall, K. Mixed-reactant, micro-tubular solid oxide fuel cells: An experimental study. *J. Power Sources* 2009, 193(1): 39–48.
68. Galloway, K. V and Sammes, N. M. Performance Degradation of Microtubular SOFCs Operating in the Intermediate-Temperature Range. *J. Electrochem. Soc.* 2009, 156(4): B526–B531.
69. Campana, R., Merino, R. I., Larrea, A., Villarreal, I. and Orera, V. M. Fabrication, electrochemical characterization and thermal cycling of anode supported microtubular solid oxide fuel cells. *J. Power Sources* 2009, 192(1): 120–125.
70. Akhtar, N., Decent, S. P. and Kendall, K. Cell temperature measurements in micro-tubular, single-chamber, solid oxide fuel cells (MT–SC–SOFCs). *J. Power Sources* 2010, 195(23): 7818–7824.
71. Suzuki, T., Zahir, M. H., Yamaguchi, T., Fujishiro, Y., Awano, M. and Sammes, N. M. Fabrication of micro-tubular solid oxide fuel cells with a single-grain-thick yttria stabilized zirconia electrolyte. *J. Power Sources* 2010, 195(23): 7825–7828.
72. Calise, F., Restuccia, G. and Sammes, N. M. Experimental analysis of performance degradation of micro-tubular solid oxide fuel cells fed by different fuel mixtures. *J. Power Sources* 2011, 196(1): 301–312.
73. Akhtar, N. and Kendall, K. Silver modified cathode for a micro-tubular, single-chamber solid oxide fuel cell. *Int. J. Hydrogen Energy* 2011, 36(1): 773–778.
74. Yamaguchi, T., Galloway, K. V., Yoon, J. and Sammes, N. M. Electrochemical characterizations of microtubular solid oxide fuel cells under a long-term testing at intermediate temperature operation. *J. Power Sources* 2011, 196(5): 2627–2630.
75. Suzuki, T., Liang, B., Yamaguchi, T., Sumi, H., Hamamoto, K. and Fujishiro, Y. One-step sintering process of gadolinia-doped ceria interlayer–scandia-stabilized zirconia electrolyte for anode supported microtubular solid oxide fuel cells. *J. Power Sources* 2012, 199: 170–173.

76. Sumi, H., Yamaguchi, T., Hamamoto, K., Suzuki, T., Fujishiro, Y., Matsui, T. and Eguchi, K. AC impedance characteristics for anode-supported microtubular solid oxide fuel cells. *Electrochim. Acta* 2012, 67: 159–165.
77. Sumi, H., Yamaguchi, T., Hamamoto, K., Suzuki, T. and Fujishiro, Y. High performance of $\text{La}_{0.6}\text{Sr}_{0.4}\text{Co}_{0.2}\text{Fe}_{0.8}\text{O}_{3-\text{x}}$ - $\text{Ce}_{0.9}\text{Gd}_{0.1}\text{O}_{1.95}$ nanoparticulate cathode for intermediate temperature microtubular solid oxide fuel cells. *J. Power Sources* 2013, 226: 354–358.
78. Suzuki, T., Liang, B., Yamaguchi, T., Sumi, H., Hamamoto, K., Fujishiro, Y. and Sammes, N. M. Performance of Ni-based Anode-Supported SOFCs with Doped Ceria Electrolyte at Low Temperatures Between 294 and 542°C. *Int. J. Appl. Ceram. Technol.* 2013, 5: 1-5.
79. Sumi, H., Yamaguchi, T., Hamamoto, K., Suzuki, T. and Fujishiro, Y. Effects of Anode Microstructure on Mechanical and Electrochemical Properties for Anode-Supported Microtubular Solid Oxide Fuel Cells. *J. Am. Ceram. Soc.* 2013, 96(11): 3584–3588.
80. Suzuki, T., Yamaguchi, T., Sumi, H., Hamamoto, K. and Fujishiro, Y. Microtubular solid-oxide fuel cells for low-temperature operation. *Mat. Res. Bull.* 2014, 39: 805–809.
81. Sumi, H., Yamaguchi, T., Hamamoto, K., Suzuki, T. and Fujishiro, Y. Electrochemical analysis for anode-supported microtubular solid oxide fuel cells in partial reducing and oxidizing conditions. *Solid State Ionics* 2014, 262: 407–410.
82. Suzuki, T., Yamaguchi, T., Sumi, H., Hamamoto, K. and Fujishiro, Y. *Low temperature operable micro-tubular SOFCS using Gd doped ceria electrolyte and Ni based anode*, Kusnezoff, M. and Bansal, N. P., Eds., Hoboken, NJ, USA: John Wiley & Sons, Inc. 2015.
83. Suzuki, T., Liang, B., Yamaguchi, T., Sumi, H., Hamamoto, K., Fujishiro, Y. and Sammes, N. M. Performance of Ni-based anode-supported SOFCs with doped ceria electrolyte at low temperatures between 294 and 542°C. *Int. J. Appl. Ceram. Technol.* 2015, 12: 358–362.
84. Sumi, H., Yamaguchi, T., Shimada, H., Hamamoto, K., Suzuki, T. Development of Ceria-Based Microtubular Solid Oxide Fuel Cells. *Trans. ECS* 2015, 69(16): 61–67.

85. Sumi, H., Kennouche, D., Yakal-kremiski, K., Suzuki, T., Barnett, S. A., Miller, D. J., Yamaguchi, T., Hamamoto, K. and Fujishiro, Y. Electrochemical and microstructural properties of Ni-(Y₂O₃)_{0.08}(ZrO₂)_{0.92}-(Ce_{0.9}Gd_{0.1})O_{1.95} anode-supported microtubular solid oxide fuel cells. *Solid State Ionics* 2016, 285: 227–233.
86. Mat, A., Canavar, M., Timurkutluk, B. and Kaplan, Y. Investigation of micro-tube solid oxide fuel cell fabrication using extrusion method. *Int. J. Hydrogen Energy* 2016, 41(23): 10037–10043.
87. Crum, A. T., Jackson, M., Halloran, J. W. and Arbor, A. *Method For Preparation of Solid State Electrochemical Device*. U.S. Patent 6,749,799B2. 2004.
88. Dhir, A. and Kendall, K. Microtubular SOFC anode optimisation for direct use on methane. *J. Power Sources* 2008, 181(2): 297–303.
89. Sun, J. J., Koh, Y. H., Choi, W. Y. and Kim, H. E. Fabrication and Characterization of Thin and Dense Electrolyte-Coated Anode Tube Using Thermoplastic Coextrusion. *J. Am. Ceram. Soc.* 2006, 89(5): 1713–1716.
90. Powell, J. and Blackburn, S. The unification of paste rheologies for the co-extrusion of solid oxide fuel cells. *J. Eur. Ceram. Soc.* 2009, 29(5): 893–897.
91. Powell, J. and Blackburn, S. Co-extrusion of multilayered ceramic micro-tubes for use as solid oxide fuel cells. *J. Eur. Ceram. Soc.* 2010, 30(14): 2859–2870.
92. Powell, J., Assabumrungrat, S. and Blackburn, S. Design of ceramic paste formulations for co-extrusion. *Powder Technol.* 2013, 245: 21–27.
93. Strathmann, H., Kock, K., Amar, P. and Baker, R. W. The formation mechanism of asymmetric membranes. *Desalination* 1975, 16(2): 179–203.
94. Tan, X., Liu, S. and Li, K. Preparation and characterization of inorganic hollow fiber membranes. *J. Memb. Sci.* 2001, 188(1): 87–95.
95. Liu, S., Tan, X., Li, K. and Hughes, R. Preparation and characterisation of SrCe_{0.95}Yb_{0.05}O_{2.975} hollow fibre membranes. *J. Memb. Sci.* 2001, 193: 249–260.
96. Liu, S., Li, K. and Hughes, R. Preparation of porous aluminium oxide (Al₂O₃) hollow fibre membranes by a combined phase-inversion and sintering method. *Ceram. Int.* 2003, 29(8): 875–881.
97. Tan, X., Liu, Y. and Li, K. Mixed conducting ceramic hollow-fiber membranes for air separation. *AIChE J.* 2005, 51(7): 1991–2000.

98. Liu, Y., Chen, O. Y., Wei, C. C. and Li, K. Preparation of yttria-stabilised zirconia (YSZ) hollow fibre membranes. *Desalination* 2006, 199(8): 360–362.
99. Liu, Y. and Li, K. Preparation of $\text{SrCe}_{0.95}\text{Yb}_{0.05}\text{O}_{3-\alpha}$ hollow fibre membranes: Study on sintering processes. *J. Memb. Sci.* 2005, 259(1-2): 47–54.
100. Wei, C. C. and Li, K. Yttria-Stabilized Zirconia (YSZ) -Based Hollow Fiber Solid Oxide Fuel Cells. *Ind. Eng. Chem. Res.* 2008, 47: 1506–1512.
101. Yin, W., Meng, B., Meng, X. and Tan, X. Highly asymmetric yttria stabilized zirconia hollow fibre membranes. *J. Alloys Compd.* 2009, 476(1-2): 566–570.
102. Grande, F. D., Thursfield, A. and Metcalfe, I. Morphological control of electroless plated Ni anodes: Influence on fuel cell performance. *Solid State Ionics* 2008, 179(35-36): 2042–2046.
103. Grande, F. D., Thursfield, A., Kanawka, K., Droushiotis, N., Doraswami, U., Li, K., Kelsall, G. and Metcalfe, I. S. Microstructure and performance of novel Ni anode for hollow fibre solid oxide fuel cells. *Solid State Ionics* 2009, 180(11-13): 800–804.
104. Kanawka, K., Grande, F. D., Wu, Z., Thursfield, A., Ivey, D., Metcalfe, I., Kelsall, G. and Li, K. Microstructure and Performance Investigation of a Solid Oxide Fuel Cells Based on Highly Asymmetric YSZ Microtubular Electrolytes. *Ind. Eng. Chem. Res.* 2010, 49(13): 6062–6068.
105. Yang, N., Tan, X., Ma, Z. and Thursfield, A. Fabrication and Characterization of $\text{Ce}_{0.8}\text{Sm}_{0.2}\text{O}_{1.9}$ Microtubular Dual-Structured Electrolyte Membranes for Application in Solid Oxide Fuel Cell Technology. *J. Am. Ceram. Soc.* 2009, 92(11): 2544–2550.
106. Yang, N., Tan, X. and Ma, Z. A phase inversion/sintering process to fabricate nickel/yttria-stabilized zirconia hollow fibers as the anode support for micro-tubular solid oxide fuel cells. *J. Power Sources* 2008, 183(1): 14–19.
107. Droushiotis, N., Doraswami, U., Kanawka, K., Kelsall, G. H. and Li, K. Characterization of NiO–yttria stabilised zirconia (YSZ) hollow fibres for use as SOFC anodes. *Solid State Ionics* 2009, 180(17-19): 1091–1099.
108. Doraswami, U., Droushiotis, N., Kelsall, G. H. Modelling effects of current distributions on performance of micro-tubular hollow fibre solid oxide fuel cells. *Electrochim. Acta* 2010, 55(11): 3766–3778.

109. Doraswami, U., Shearing, P., Droushiotis, N., Li, K., Brandon, N. P., Kelsall, G. H. Modelling the effects of measured anode triple-phase boundary densities on the performance of micro-tubular hollow fiber SOFCs. *Solid State Ionics* 2011, 192(1): 494–500.
110. Yang, C., Jin, C., Liu, M. and Chen, F. Intermediate temperature micro-tubular SOFCs with enhanced performance and thermal stability. *Electrochemistry Communications*. 2013, 34: 231–234.
111. Jin, C., Yang, C. and Chen, F. Effects on microstructure of NiO–YSZ anode support fabricated by phase-inversion method. *J. Memb. Sci.* 2010, 363(1-2): 250–255.
112. Zhao, F., Jin, C., Yang, C., Wang, S. and Chen, F. Fabrication and characterization of anode-supported micro-tubular solid oxide fuel cell based on $\text{BaZr}_{0.1}\text{Ce}_{0.7}\text{Y}_{0.1}\text{Yb}_{0.1}\text{O}_{3-\delta}$ electrolyte. *J. Power Sources* 2011, 196(2): 688–691.
113. Zhou, D., Peng, S., Wei, Y., Li, Z. and Wang, H. Novel asymmetric anode-supported hollow fiber solid oxide fuel cell. *J. Alloys Compd.* 2012, 523: 134–138.
114. Droushiotis, N., Othman, M. H. D., Doraswami, U., Li, K. and Kelsall, G. Co-Extrusion/Phase Inversion/Co-Sintering for Fabrication of Hollow Fiber Solid Oxide Fuel Cells. *ECS Trans.* 2009, 25(2): 665–672.
115. Droushiotis, N., Doraswami, U., Ivey, D., Othman, M. H. D., Li, K. and Kelsall, G. Fabrication by Co-extrusion and electrochemical characterization of micro-tubular hollow fibre solid oxide fuel cells. *Electrochem. commun.* 2010, 12(6): 792–795.
116. Othman, M. H. D., Droushiotis, N., Wu, Z., Kelsall, G. and Li, K. High-Performance, Anode-Supported, Microtubular SOFC Prepared from Single-Step-Fabricated, Dual-Layer Hollow Fibers. *Adv. Mater.* 2011, 23: 2480–2483.
117. Othman, M. H. D., Droushiotis, N., Wu, Z., Kanawka, K., Kelsall, G. and Li, K. Electrolyte thickness control and its effect on electrolyte/anode dual-layer hollow fibres for micro-tubular solid oxide fuel cells. *J. Memb. Sci.* 2010, 365(1-2): 382–388.
118. Kanawka, K., Othman, M. H. D., Droushiotis, N., Wu, Z., Kelsall, G. and Li, K. NI/Ni-YSZ Current Collector/Anode Dual Layer Hollow Fibers for Micro-Tubular Solid Oxide Fuel Cells. *Fuel Cells* 2011, 11(5): 690–696.

119. Li, T., Wu, Z. and Li, K. Single-step fabrication and characterisations of triple-layer ceramic hollow fibres for micro-tubular solid oxide fuel cells (SOFCs). *J. Memb. Sci.* 2014, 449: 1–8.
120. Li, T., Wu, Z. and Li, K. Co-extrusion of electrolyte/anode functional layer/anode triple-layer ceramic hollow fibres for micro-tubular solid oxide fuel cells-electrochemical performance study. *J. Power Sources* 2015, 273: 999–1005.
121. Wei, C.C. Yttria stabilised zirconia (YSZ) membranes and their applications Ph.D thesis, Imperial College London, 2009.
122. Jin, C., Liu, J., Li, L. and Bai, Y. Electrochemical properties analysis of tubular NiO–YSZ anode-supported SOFCs fabricated by the phase-inversion method. *J. Memb. Sci.* 2009, 341(1-2): 233–237.
123. Yang, C., Li, W., Zhang, S., Bi, L., Peng, R., Chen, C. and Liu, W. Fabrication and characterization of an anode-supported hollow fiber SOFC. *J. Power Sources* 2009, 187(1): 90–92.
124. Yang, C., Jin, C. and Chen, F. Micro-tubular solid oxide fuel cells fabricated by phase-inversion method. *Electrochem. commun.* 2010, 12(5): 657–660.
125. Zhang, X., Lin, B., Ling, Y., Dong, Y., Meng, G., Liu, X. and Zhao, L. An anode-supported micro-tubular solid oxide fuel cell with redox stable composite cathode. *Int. J. Hydrogen Energy* 2010, 35(16): 8654–8662.
126. Yang, C., Jin, C. and Chen, F. Performances of micro-tubular solid oxide cell with novel asymmetric porous hydrogen electrode. *Electrochim. Acta* 2010, 56(1): 80–84.
127. Droushiotis, N., Othman, M. H. D., Doraswami, U., Wu, Z., Kelsall, G. and Li, K. Novel co-extruded electrolyte–anode hollow fibres for solid oxide fuel cells. *Electrochem. commun.* 2009, 11(9): 1799–1802.
128. Meng, X., Gong, X., Yin, Y., Yang, N. T., Tan, X. and Ma, Z. F. Microstructure tailoring of YSZ/Ni-YSZ dual-layer hollow fibers for micro-tubular solid oxide fuel cell application. *Int. J. Hydrogen Energy* 2013, 38(16): 6780–6788.
129. Yang, C., Ren, C., Yu, L. and Jin, C. High performance intermediate temperature micro-tubular SOFCs with $\text{Ba}_{0.9}\text{Co}_{0.7}\text{Fe}_{0.2}\text{Nb}_{0.1}\text{O}_{3-\delta}$ as cathode. *Int. J. Hydrogen Energy* 2013, 38(35): 15348–15353.

130. Meng, X., Gong, X., Yang, N., Yin, Y. and Tan, X. Carbon-resistant Ni-YSZ / Cu-CeO₂-YSZ dual-layer hollow fiber anode for micro tubular solid oxide fuel cell. *Int. J. Hydrogen Energy* 2014, 39(8): 3879–3886.
131. Yang, N., Meng, X., Tan, X. and Ma, Z. F. Dual-layer LSM-YSZ/LSM hollow fiber for micro tublar SOFC with a functional cathode. *Electrochemical Conference on Energy & the Environment (ECEE)*, Mac 16, 2014. The Electrochemical Society, 2014.
132. Meng, X., Gong, X., Yin, Y., Yang, N., Tan, X. and Ma, Z. F. Effect of the co-spun anode functional layer on the performance of the direct-methane microtubular solid oxide fuel cells. *J. Power Sources* 2014, 247: 587–593.
133. Meng, X., Yang, N., Gong, X., Yin, Y., Ma, Z. F., Tan, X., Shao, Z. and Liu, S. Novel cathode-supported hollow fibers for light weight micro-tubular solid oxide fuel cells with an active cathode functional layer. *J. Mater. Chem. A* 2015, 3: 1017–1022.
134. Meng, X., Yan, W., Yang, N., Tan, X. and Liu, S. Highly stable microtubular solid oxide fuel cells based on integrated electrolyte/anode hollow fibers. *J. Power Sources* 2015, 275: 362–369.
135. Liu, T., Wang, Y., Ren, C., Fang, S., Mao, Y. and Chen, F. Novel light-weight, high-performance anode-supported microtubular solid oxide fuel cells with an active anode functional layer. *J. Power Sources* 2015, 293: 852–858.
136. Ren, C., Wang, S., Liu, T., Lin, Y. and Chen, F. Fabrication of micro-tubular solid oxide fuel cells using sulfur-free polymer binder via a phase inversion method. *J. Power Sources* 2015, 290: 1–7.
137. Ren, C., Liu, T., Maturavongsadit, P., Luckanagul, J. A. and Chen, F. Effect of PEG additive on anode microstructure and cell performance of anode-supported MT-SOFCs fabricated by phase inversion method. *J. Power Sources* 2015, 279: 774–780.
138. Li, T., Wu, Z. and Li, K. High-efficiency, nickel-ceramic composite anode current collector for micro-tubular solid oxide fuel cells. *J. Power Sources* 2015, 280: 446–452.
139. Jamil, S. M., Othman, M. H. D., Rahman, M. A., Jaafar, J. and Ismail, A. F. Anode supported micro-tubular SOFC fabricated with mixed particle size electrolyte via phase-inversion technique. *Int. J. Hydrogen Energy* 2016, In Press: 1–14.

140. Ahmad, S. H., Jamil, S. M., Othman, M. H. D., Rahman, M. A., Jaafar, J. and Ismail, A. F. Co-extruded dual-layer hollow fiber with different electrolyte structure for a high temperature micro-tubular solid oxide fuel cell. *Int. J. Hydrogen Energy* 2016, In Press: 1–9.
141. Okawa, Y. and Hirata, Y. Sinterability, microstructures and electrical properties of Ni/Sm-doped ceria cermet processed with nanometer-sized particles. *J. Eur. Ceram. Soc.* 2005, 25(4): 473–480.
142. Gil, V., Tartaj, J. and Moure, C. Low temperature synthesis and sintering behaviour of Gd-doped ceria nanosized powders: comparison between two synthesis procedures. *Bol. Soc. Esp. Ceram.* 2009, 48(2): 69–76.
143. Han, M., Liu, Z., Zhou, S. and Yu, L. Influence of Lithium Oxide Addition on the Sintering Behavior and Electrical Conductivity of Gadolinia Doped Ceria. *J. Mater. Sci. Technol.* 2011, 27(5): 460–464.
144. Tok, A. I. Y., Luo, L. H. and Boey, F. Y. C. Carbonate Co-precipitation of Gd₂O₃-doped CeO₂ solid solution nano-particles. *Mater. Sci. Eng. A* 2004, 383(2): 229–234.
145. Prasad, D. H., Jung, H. Y., Jung, H. G., Kim, B. K., Lee, H. W. and Lee, J. H. Single step synthesis of nano-sized NiO-Ce_{0.75}Zr_{0.25}O₂ composite powders by glycine nitrate process. *Mater. Lett.* 2008, 62(4-5): 587–590.
146. Prasad, D. H., Son, J. W., Kim, B. K., Lee, H. W. and Lee, J. H. Synthesis of nano-crystalline Ce_{0.9}Gd_{0.1}O_{1.95} electrolyte by novel sol-gel thermolysis process for IT-SOFCs. *J. Eur. Ceram. Soc.* 2008, 28(16): 3107–3112.
147. Prasad, D. H., Kim, H.R., Park, J. S., Son, J. W., Kim, B. K., Lee, H. W. and Lee, J. H. Superior sinterability of nano-crystalline gadolinium doped ceria powders synthesized by co-precipitation method. *J. Alloys Compd.* 2010, 495(1): 238–241.
148. Kausch, H., Fesko, D. and Tschoegl, N. The random packing of circles in a plane. *J. Colloid Interface Sci.* 1971, 37(3): 603–611.
149. Bideau, D. and Troadec, J. P. Compacity and mean coordination number of dense packings of hard discs. *J Phys C Solid State Phys.* 1984, 17: 731–735.
150. Kleinlogel, C. M. and Gauckler, L. J. Mixed Electronic-Ionic Conductivity of Cobalt Doped Cerium Gadolinium Oxide. *J. Electroceramics* 2000, 3(5): 231–243.

151. Jud, E., Huwiler, C. B. and Gauckler, L. J. Grain Growth of Micron-sized Grains in Undoped and Cobalt oxide doped Ceria Solid Solutions. *J Am Ceram Soc Japan* 2006, 114(11): 963–969.
152. Jud, E. and Gauckler, L. J. Sintering Behavior of In Situ Cobalt Oxide-Doped Cerium-Gadolinium Oxide Prepared by Flame Spray Pyrolysis. *J. Am. Ceram. Soc.* 2006, 89(9): 2970–2973.
153. Jud, E. and Gauckler, L. J. Sintering Behavior of Cobalt Oxide Doped Ceria Powders of Different Particle Sizes. *J. Electroceramics* 2005, 14(3): 247–253.
154. Pérez -Coll, D., Núñez, P., Marrero-Lopez, D., Abrantes, J. C. C. and Frade, J. R. Effects of sintering additives on the mixed transport properties of ceria-based materials under reducing conditions. *J. Solid State Electrochem.* 2004, 8(9): 644–649.
155. Pérez-Coll, D., Núñez, P., Ruiz-Morales, J. C., Peña-Martínez, J. and Frade, J. R. Re-examination of bulk and grain boundary conductivities of $Ce_{1-x}Gd_xO_{2-\delta}$ ceramics. *Electrochim. Acta* 2007, 52(5): 2001–2008.
156. Prasad, D. H., Park, S. Y., Ji, H., Kim, H. R., Son, J. W., Kim, B. K., Lee, H. W. and Lee, J. H. Cobalt oxide co-doping effect on the sinterability and electrical conductivity of nano-crystalline Gd-doped ceria. *Ceram. Int.* 2012, 38: S497–S500.
157. Taub, S., Neuhaus, K., Wiemhöfer, H. D., Ni, N., Kilner, J. A. and Atkinson, A. The effects of Co and Cr on the electrical conductivity of cerium gadolinium oxide. *Solid State Ionics* 2015, 282: 54–62.
158. Clarkson, M. O., Wood, R. A., Lenton, T. M., Daines, S. J., Richoz, S., Ohnemüller, F., Meixner, A., Poulton, S. W. and Tipper, E. T. Sintering Mechanism of CuO-doped $Ce_{0.8}Gd_{0.2}O_{2-\delta}$ Ceramics. *ECS Trans.* 2007, 7(1): 2269- 2276.
159. Dong, Y., Hampshire, S., Zhou, J. and Meng, G. Synthesis and sintering of Gd-doped CeO₂ electrolytes with and without 1at.% CuO doping for solid oxide fuel cell applications. *Int. J. Hydrogen Energy* 2011, 36(8): 5054–5066.
160. Lima, C. G. M., Santos, T. H., Grilo, J. P. F., Dutra, R. P. S., Nascimento, R. M., Rajesh, S., Fonseca, F. C. and Macedo, D. A. Synthesis and properties of CuO-doped $Ce_{0.9}Gd_{0.1}O_{2-\delta}$ electrolytes for SOFCs. *Ceram. Int.* 2015, 41(3): 4161–4168.

161. Zhang, T. S., Hing, P., Huang, H. and Kilner, J. A. The effect of Fe doping on the sintering behavior of commercial CeO₂ powder. *J. Mater. Process. Technol.* 2001, 113: 463–468.
162. Zhang, T. S., Hing, P., Huang, H. and Kilner, J. A. Early-stage sintering mechanisms of Fe-doped CeO₂. *J. Mater. Sci.* 2002, 37(5): 997–1003.
163. Zhang, T. S., Ma, J., Kong, L. B., Zeng, Z. Q., Hing, P. and Kilner, J. A. Final-stage sintering behavior of Fe-doped CeO₂. *Mater. Sci. Eng. B Solid-State Mater. Adv. Technol.* 2003, 103(2): 177–183.
164. Zhang, T. S., Ma, J., Chan, S. H. and Kilner, J. A. Grain boundary conduction of Ce_{0.9}Gd_{0.1}O_{2-δ} ceramics derived from oxalate coprecipitation: Effects of Fe loading and sintering temperature. *Solid State Ionics* 2005, 176(3-4): 377–384.
165. Zhang, T. S., Hing, P., Huang, H. and Kilner, J. A. Sintering study on commercial CeO₂ powder with small amount of MnO₂ doping. *Mater. Lett.* 2002, 57: 507–512.
166. Kleinlogel, C. M. and Gauckler, L. J. Sintering and properties of nanosized ceria solid solutions. *Solid State Ionics* 2000, 135: 567–573.
167. Kleinlogel, C. and Gauckler, L. J. Sintering of Nanocrystalline CeO₂ Ceramics. *Adv. Mater.* 2001, 13(14): 1081–1085.
168. Zhang, T. S., Hing, P., Huang, H. and Kilner, J. A. Sintering and densification behavior of Mn-doped CeO₂. *Mater. Sci. Eng. B* 2001, 83: 235–241.
169. Zhang, T. S., Hing, P. and Huang, H. Sintering of Co-doped CeO₂ powder. *J. Mater. Sci. Lett.* 2002, 21: 75–77.
170. Zhang, T. S., Hing, P., Huang, H. and Kilner, J. A. Sintering and grain growth of CoO-doped CeO₂ ceramics. *J. Eur. Ceram. Soc.* 2002, 22: 27–34.
171. Zhang, T. S., Zeng, Z. Q., Huang, H., Hing, P. and Kilner, J. A. Effect of alumina addition on the electrical and mechanical properties of Ce_{0.8}Gd_{0.2}O_{2-δ} ceramics. *Mater. Lett.* 2002, 57: 124–129.
172. Cho, P., Lee, B., Kim, D., Lee, J., Kim, D. and Park, H. Improvement of Grain-Boundary Conduction in Gadolinia-Doped Ceria by the Addition of CaO. *Electrochem. Solid-State Lett.* 2006, 9(9): 399–402.
173. Li, B., Wei, X. and Pan, W. Electrical properties of Mg-doped Ce_{0.9}Gd_{0.1}O_{1.95} under different sintering conditions. *J. Power Sources* 2008, 183(2): 498–505.

174. Gil, V., Tartaj, J., Moure, C. and Duran, P. Rapid densification by using Bi_2O_3 as an aid for sintering of gadolinia-doped ceria ceramics. *Ceram. Int.* 2007, 33(3): 471–475.
175. Gil, V., Tartaj, J., Moure, C. and Duran, P. Effect of Bi_2O_3 addition on the sintering and microstructural development of gadolinia-doped ceria ceramics. *J. Eur. Ceram. Soc.* 2007, 27(2-3): 801–805.
176. Ge, L., Li, R., He, S., Chen, H. and Guo, L. Enhanced grain-boundary conduction in polycrystalline $\text{Ce}_{0.8}\text{Gd}_{0.2}\text{O}_{1.9}$ by zinc oxide doping: Scavenging of resistive impurities. *J. Power Sources* 2013, 230: 161–168.
177. Villas-Boas, L. A., Figueiredo, F. M. L., De Souza, D. P. F. and Marques, F. M. B. Zn as sintering aid for ceria-based electrolytes. *Solid State Ionics* 2014, 262: 522–525.
178. Zhu, T., Lin, Y., Yang, Z., Su, D., Ma, S., Han, M. and Chen, F. Evaluation of Li_2O as an efficient sintering aid for gadolinia-doped ceria electrolyte for solid oxide fuel cells. *J. Power Sources* 2014, 261: 255–263.
179. Lee, J. A., Lee, Y. E., Lee, H. C., Heo, Y. W., Lee, J. H. and Kim, J. J. Effect of Li_2O content and sintering temperature on the grain growth and electrical properties of Gd-doped CeO_2 ceramics. *Ceram. Int.* 2016, 42(9): 11170–11176.
180. Seo, S. W., Park, M. W. and Lee, J. S. Effects of Lithium Oxide Addition on Sintering Behavior and Electrical Conductivity of $\text{Ce}_{0.8}\text{Gd}_{0.2}\text{O}_{1.9}$ Ceramics Prepared by Commercial Powders. *J. Nanosci. Nanotechnol.* 2016, 16(5): 5320–5323.
181. Nicholas, J. D. and Dejonghe, L. Prediction and evaluation of sintering aids for Cerium Gadolinium Oxide. *Solid State Ionics* 2007, 178(19-20): 1187–1194.
182. Nicholas, J. D. Low Temperature Constrained Sintering of Cerium Gadolinium Oxide Films for Solid Oxide Fuel Cell Applications, Ph.D thesis, University of California, Berkeley: Lawrence Berkeley National Laboratory. 2007.
183. Nicholas J. D. and Dejonghe, L. C. Creating Dense, Constrained $\text{Ce}_{0.9}\text{Gd}_{0.1}\text{O}_{1.95}$ Films at Low Temperature for SOFC Applications. *Mater. Res. Soc. Symp. Proc.* 2007, Materials Research Society, 2007, 1023: JJ05-09.
184. Esposito, V., Zunic, M. and Traversa, E. Improved total conductivity of nanometric samaria-doped ceria powders sintered with molten LiNO_3 additive. *Solid State Ionics* 2009, 180(17-19): 1069–1075.

185. Li, S., Xian, C., Yang, K., Sun, C., Wang, Z. and Chen, L. Feasibility and mechanism of lithium oxide as sintering aid for $\text{Ce}_{0.8}\text{Sm}_{0.2}\text{O}_\delta$ electrolyte. *J. Power Sources* 2012, 205: 57–62.
186. Manakor, K., Jamil, S. M., Othman, M. H. D., Rahman, M. A., Jaafar, J. and Ismail, A. F. Effect of Sintering Aid on CGO Electrolyte for the Fabrication of Low Cost, *J. Teknol.* 2014, 2: 33–39.
187. Lee, J. S., Choi, K. H., Ryu, B. K., Shin, B. C. and Kim, I. S. Effects of alumina additions on sintering behavior of gadolinia-doped ceria. *Ceram. Int.* 2004, 30: 807–812.
188. Iqbal, A., Ani, I. and Rajput, R. Performance of microwave synthesized dual solvent dope solution and lithium bromide additives on poly(ethersulfone) membranes. *J. Chem. Technol. Biotechnol.* 2012, 87: 177–188.
189. Liu, S. and Li, K. Preparation $\text{TiO}_2/\text{Al}_2\text{O}_3$ composite hollow fibre membranes. *J. Memb. Sci.* 2003, 218(1-2): 269–277.
190. Boldrin, P., Ruiz-Trejo, E., Yu, J., Gruar, R. I., Tighe, C. J., Chang, K. C., Ilavsky, J., Darr, J. A. and Brandon, N. Nanoparticle scaffolds for syngas-fed solid oxide fuel cells. *J. Mater. Chem. A* 2015, 3(6): 3011–3018.
191. Mohamed, M. A., Salleh, W. W. N., Jaafar, J., Ismail, A. F., Mutalib, M. A., Sani, N. A. A., M. Asri, S. E. A. and Ong, C. S. Physicochemical characteristic of regenerated cellulose/N-doped TiO_2 nanocomposite membrane fabricated from recycled newspaper with photocatalytic activity under UV and visible light irradiation. *Chem. Eng. J.* 2016, 284: 202–215.
192. Xia, H., Wang, Y., Lin, J. and Lu, L. Hydrothermal synthesis of MnO_2/CNT nanocomposite with a CNT core/porous MnO_2 sheath hierarchy architecture for supercapacitors. 2012, 7(33): 1–10.
193. Bagheri, S., Hir, Z. A. M., Yousefi, A. T. and Hamid, S. B. A. Progress on mesoporous titanium dioxide: Synthesis, modification and applications. *Microporous Mesoporous Mater.* 2014, 218: 206–222.
194. Sonwane, C. G. and Bhatia, S. K. Characterization of Pore Size Distributions of Mesoporous Materials from Adsorption Isotherms. *J. Phys. Chem. B* 2000, 104: 9099–9110.
195. Sinha, A. K. and Suzuki, K. Preparation and characterization of novel mesoporous ceria-titania. *J. Phys. Chem. B* 2005, 109(5): 1708–1714.

196. Balbuenat, P. B. and Gubbins, K. E. Theoretical Interpretation of Adsorption Behavior of Simple Fluids in Slit Pores. *Am. Chem. Soc.* 1993, 9(4): 1801–1814.
197. Bhambhani, M. R., Cutting, P. A., Sing, K. S. W. and Turk, D. H. Analysis of Nitrogen Adsorption Isotherms on Porous and Nonporous Silicas by the BET and α Methods. *J. Colloid Interface Sci.* 1970, 38(1): 109-117.
198. Mohamed, M. A., Salleh, W. N. W., Jaafar, J., Ismail, A. F. and Tanemura, M. Regenerated cellulose membrane as bio-template for in-situ growth of visible-light driven C-modified mesoporous titania. *Carbohydr. Polym.* 2016, 146: 166–173.
199. Kara, A., Demirbel, E., Tekin, N., Osman, B. and Beşirli, N. Magnetic vinylphenyl boronic acid microparticles for Cr(VI) adsorption: Kinetic, isotherm and thermodynamic studies. *J. Hazard. Mater.* 2015, 286: 612–623.
200. Liu, Y., Hao, X., Wang, Z., Wang, J., Qiao, J., Yan, Y. and Sun, K. A novel sintering method to obtain fully dense gadolinia doped ceria by applying a direct current. *J. Power Sources* 2012, 215: 296–300.
201. Huang, K., Feng, M. and Goodenough, J. B. Synthesis and electrical properties of dense $\text{Ce}_{0.9}\text{Gd}_{0.1}\text{O}_{1.95}$ ceramics. *J. Am. Ceram. Soc.* 1998, 81(2): 357–362.
202. Ruiz, M. L., Lick, I. D., Ponzi, M. I., Castellón, E. R., Jiménez-López, A. and Ponzi, E. N. Thermal decomposition of supported lithium nitrate catalysts. *Thermochim. Acta* 2010, 499(1-2): 21–26.
203. Datta, P., Majewski, P. and Aldinger, F. Study of gadolinia-doped ceria solid electrolyte surface by XPS. *Mater. Charact.* 2009, 60(2): 138–143.
204. Wang, Q., Jiang, Z., Wang, Y., Chen, D. and Yang, D. Photocatalytic properties of porous C-doped TiO_2 and Ag/C-doped TiO_2 nanomaterials by eggshell membrane templating. *J Nanopart Res* 2009, 11: 375–384.
205. Gautier, J. L., Rios, E., Gracia, M., Marco, J. F. and Gancedo, J. R. Characterisation by X-ray photoelectron spectroscopy of thin $\text{Mn}_x\text{Co}_{3-x}\text{O}_4$ ($1 \geq x \geq 0$) spinel films prepared by low-temperature spray pyrolysis. *Thin Solid Films* 1997, 311: 51–57.
206. Gamage, J., Cui, W. and Zhang, Z. Degradative and disinfective properties of carbon-doped anatase – rutile TiO_2 mixtures under visible light irradiation. *Catal. Today* 2013, 207: 191–199.

207. Mohamed, M. A., Salleh, W. N. W., Jaafar, J. and Ismail, A. F. Structural characterization of N-doped anatase–rutile mixed phase TiO₂ nanorods assembled microspheres synthesized by simple sol–gel method. *J. Sol-Gel Sci. Technol.* 2015, 74(2): 513–520.
208. Feijoo, P. C., Pampillón, M. A., San Andrés, E. and Lucía, M. L. Optimization of scandium oxide growth by high pressure sputtering on silicon. *Thin Solid Films* 2012, 526(2013): 81–86.
209. Lademan, W., See, A. K., and Klebanoff, L. E., Multiplet structure in high-resolution and spin-resolved x-ray photoemission from gadolinium. *Phys. Rev. B* 1996, 54(23): 17191–17198.
210. Chen, H., Sayari, A. and Adnot, A. Composition activity effects of Mn–Ce–O composites on phenol catalytic wet oxidation. *Appl. Catal. B Environ.* 2001, 32: 195–204.
211. Yao, H. C., Zhao, X. L., Chen, X., Wang, J. C., Ge, Q. Q., Wang, J. S. and Li, Z. J. Processing and characterization of CoO and Sm₂O₃ codoped ceria solid solution electrolyte. *J. Power Sources* 2012, 205: 180–187.
212. Aduru, S., Contarini, S. and Rabalais, J. W. Electron-, X-ray-, and Ion-Stimulated Decomposition of Nitrate Salts. *J. Phys. Chem.* 1986, 90: 1683–1688.
213. Chia-ching, W. and Cheng-fu, Y. Investigation of the properties of nanostructured Li-doped NiO films using the modified spray pyrolysis method. 2013, 8(33): 2–6.
214. Chen, Y., Lee, C., Yeng, M. and Chiu, H. The effect of calcination temperature on the crystallinity of TiO₂ nanopowders. *J. Cryst. Growth* 2003, 247: 363–370.
215. Wang, Z., Kale, G. M. and Ghadiri, M. Synthesis and characterization of Ce_xGd_{1-x}O_{2-δ} nanopowders employing an alginate mediated ion-exchange process. *Chem. Eng. J.* 2012, 198-199: 149–153.
216. Martínez, J. M. G., Meneses, R. A. M., and Silva, C. R. M., Gonzalez Martinez, J. M., Munoz Meneses, R. A., da Silva, C. R. M. Synthesis of Gadolinium Doped Ceria Ceramic Powder by Polymeric Precursor Method (Pechini). *Brazilian Ceram. Conf. 57* 2014, 798-799: 182–188.

217. Sulaiman, M., Dzulkarnain, N. A., Rahman, A. A. and Mohamed, N. S. Sol-gel synthesis and characterization of $\text{LiNO}_3\text{-Al}_2\text{O}_3$ composite solid electrolyte. *Solid State Sci.* 2012, 14(1): 127–132.
218. Ruiz, M. L., Lick, I. D., Ponzi, M. I. and Ponzi, E. N. Catalysts of alkaline nitrates supported on oxides for the diesel soot combustion. Deactivation by hydro-treatment and CO_2 . *Catal. Commun.* 2013, 34(2): 45–51.
219. Cavanagh, A. S. S., Lee, Y., Yoon, B. and George, S. M. M., Transactions, E. C. S., Society, T. E. Atomic Layer Deposition of LiOH and Li_2CO_3 Using Lithium t-Butoxide as the Lithium Source. *ECS Trans.* 2010, 33(2): 223–229.
220. Rappoport, I. M. Z. *The chemistry of organolithium compounds Part 1*, Z. Rappoport, I. M., Ed., West Sussex, England: John Wiley & Sons, Ltd, 2004.
221. Praserthdam, P., Phungphadung, J. and Tanakulrungsank, W. Effect of crystallite size and calcination temperature on the thermal stability of single nanocrystalline chromium oxide: Expressed by novel correlation. *Mater. Res. Innov.* 2003, 7(2): 118–123.
222. Zhang, W., Kuhn, L. T., Joergensen, P. S., Sudireddy, B. R., Bentzen, J. J., Bernuy-Lopez, C., Veltze, S. and Ramos, T. Instability and growth of nanoscale $\text{Ce}_{0.8}\text{Gd}_{0.2}\text{O}_{1.9}/\text{NiO}$ infiltrate in $\text{Sr}_{0.94}\text{Ti}_{0.9}\text{Nb}_{0.1}\text{O}_3\text{-Zr}_{0.84}\text{Y}_{0.16}\text{O}_{1.92}$ anodes for solid oxide fuel cells. *J. Power Sources* 2014, 258: 297–304.
223. Burbano, M., Nadin, S., Marrocchelli, D., Salanne, M. and Watson, G. W. Ceria co-doping: synergistic or average effect. *Phys. Chem. Chem. Phys.* 2014, 16(18): 8320–8331.
224. Othman, M. H. D., Droushiotis, N., Wu, Z., Kelsall, G. and Li, K. Novel fabrication technique of hollow fibre support for micro-tubular solid oxide fuel cells. *J. Power Sources* 2011, 196: 5035–5044.
225. Kingsbury, B. F. K. and Li, K. A morphological study of ceramic hollow fibre membranes. *J. Memb. Sci.* 2009, 328(1-2): 134–140.
226. Kingsbury, B. F. K. A Morphological Study of Ceramic Hollow Fibre Membranes: A Perspective on Multifunctional Catalytic Membrane Reactor, Ph.D thesis, Imperial College London, 2010.
227. Yu, F., Xiao, J., Lei, L., Cai, W., Zhang, Y., Liu, J. and Liu, M. Effects of doping alumina on the electrical and sintering performances of yttrium-stabilized-zirconia. *Solid State Ionics* 2016, 289: 28–34.

228. Huijsmans, J. P. P. Ceramics in solid oxide fuel cells. *Curr. Opin. Solid State Mater. Sci.* 2001, 5(4): 317–323.
229. Zhang, T. S., Ma, J., Kong, L. B., Hing, P. and Kilner, J. A. Preparation and mechanical properties of dense $\text{Ce}_{0.8}\text{Gd}_{0.2}\text{O}_{2-\delta}$ ceramics. *Solid State Ionics* 2004, 167(1-2): 191–196.
230. Lee, J. The impact of anode microstructure on the power generating characteristics of SOFC. *Solid State Ionics* 2003, 158(3-4): 225–232.
231. Sarikaya, A., Petrovsky, V. and Dogan, F. Effect of the anode microstructure on the enhanced performance of solid oxide fuel cells. *Int. J. Hydrogen Energy* 2012, 37(15): 11370–11377.
232. Choi, Y. G., Park, J. Y., Song, H., Kim, H. R., Son, J. W., Lee, J. H., Je, H. J., Kim, B. K., Lee, H. W. and Yoon, K. J. Microstructure–polarization relations in nickel/ gadolinia-doped ceria anode for intermediate-temperature solid oxide fuel cells. *Ceram. Int.* 2013, 39(15): 4713–4718.
233. Bissett, H., Zah, J. and Krieg, H. M. Manufacture and optimization of tubular ceramic membrane supports. *Powder Technol.* 2008, 181(1): 57–66.
234. Tanner, C. W., Fung, K. Z. and Virkar, A. V. The Effect of Porous Composite Electrode Structure on Solid Oxide Fuel Cell Performance. *J. Electrochem. Soc.* 1997, 144(1): 21–30.
235. Vohs, J. M., Gorte, R. J. High-performance SOFC cathodes prepared by infiltration. *Adv. Mater.* 2009, 21(9): 943–956.
236. Virkar, A. V., Chen, J., Tanner, C. W. and Kim, J. W. Role of electrode microstructure on activation and concentration polarizations in solid oxide fuel cells. *Solid State Ionics* 2000, 131(1): 189–198.
237. Yu, H.-C., Zhao, F., Virkar, A. V. and Fung, K. Z. Electrochemical characterization and performance evaluation of intermediate temperature solid oxide fuel cell with $\text{La}_{0.75}\text{Sr}_{0.25}\text{CuO}_{2.5-\delta}$ cathode. *J. Power Sources* 2005, 152: 22–26.
238. Zhang, L., Zhu, L. and Virkar, A. V. Electronic conductivity measurement of yttria-stabilized zirconia solid electrolytes by a transient technique. *J. Power Sources* 2016, 302: 98–106.
239. Zhao, F. and Virkar, A. V. Dependence of polarization in anode-supported solid oxide fuel cells on various cell parameters. *J. Power Sources* 2005, 141(1): 79–95.

240. Droushiotis, N., Grande, F. D., Othman, M. H. D., Kanawka, K., Doraswami, U., Metcalfe, I., Li, K. and Kelsall, G. Comparison Between Anode-Supported and Electrolyte-Supported Ni-CGO-LSCF Micro-tubular Solid Oxide Fuel Cells. *Fuel Cells* 2014, 14(2): 200–211.
241. Ahn, J. S., Pergolesi, D., Camaratta, M. A., Yoon, H., Lee, B. W., Lee, K. T. and Jung, D. W., Traversa, E. and Wachsman, E. D. High-performance bilayered electrolyte intermediate temperature solid oxide fuel cells. *Electrochem. commun.* 2009, 11(7): 1504–1507.
242. Yamaguchi, T., Shimizu, S., Suzuki, T., Fujishiro, Y. and Awano, M. Evaluation of Micro LSM-Supported GDC/ScSZ Bilayer Electrolyte with LSM–GDC Activation Layer for Intermediate Temperature-SOFCs. *J. Electrochem. Soc.* 2008, 155(4): B423-B426.
243. Kim, H. J., Kim, M., Neoh, K. C., Han, G. D., Bae, K., Shin, J. M., Kim, G. T. and Shim, J. H. Slurry spin coating of thin film yttria stabilized zirconia/gadolinia doped ceria bi-layer electrolytes for solid oxide fuel cells. *J. Power Sources* 2016, 327: 401–407.